TEMPERATURE AND VELOCITY DISTRIBUTION IN NON-UNIFORM TURBULENT FLOW

Thesis by

Virgil Jennings Berry, Jr.

In Partial Fulfillment of the Requirements

For the Degree of

Doctor of Philosophy

California Institute of Technology

Pasadena, California

1951

Acknowledgment

Financial assistance for this research was obtained from the California Institute of Technology. The entire program was under the direction of Professor B. H. Sage, and his guidance and constant encouragement are gratefully acknowledged. Much credit is due D. M. Mason and W. G. Schlinger who gave generously and willingly of their time in many discussions, and Professor W. N. Lacey whose comments regarding the preparation of the manuscript were invaluable. The experimental data were obtained with the cooperation of D. K. Breaux, S. D. Cavers, J. L. Mason, and R. M. Stewart. W. G. Schlinger and R. H. MacNeal contributed greatly to the successful prosecution of the analog computer work. The helpful assistance of Institute employees in the construction of the equipment used and in the performance of the calculations is appreciated. Virginia Berry prepared many of the figures.

Special credit is due Alice Berry for her untiring efforts both in the typing and in the assembling of the manuscript.

Abstract

As part of a series of investigations of the relative rates of transfer of heat and momentum in a turbulent air stream, measurements were made of temperature and air speed distributions in the wake of an 0.0318 inch diameter steel cylinder. The cylinder was electrically heated and was mounted transverse to a two-dimensional, turbulently flowing air stream. Vertical traverses were made at seven stations downstream from the cylinder at each of three bulk air speeds. The data are presented in both graphical and tabular form. Measurements were also made of the rate of heat transfer from the cylinder as a function of average cylinder surface temperature.

The analytical problem of predicting temperature and air speed profiles downstream from a heated cylinder is considered, and a number of simple correlations are derived. These correlations are shown to describe the data with accuracy, and are extended to the prediction of temperatures in the wake of a large heated cylinder and in the wake of a heated sphere, and to the prediction of concentrations in a turbulent diffusion flame apparatus. Agreement with experiment is excellent.

An electric analog computer was used to calculate temperature distributions in a uniformly flowing turbulent air stream for three different sets of temperature boundary conditions. The resulting profiles compare favorably with available experimental data.

Table of Contents

Introduction

For a number of years the design of heat and mass exchanging equipment has been based upon overall transfer correlations (1,2,3). However, since modern technological advances have presented more exacting design problems, the ability to predict values of temperature, concentration, and velocity at a point in a fluid is often necessary in systems involving turbulent transfer. During the past five years an experimental program designed to yield information on the relative rates of transfer of heat, material, and momentum in a turbulent air stream has been conducted in the Chemical Engineering Laboratories of the California Institute of Technology. The ultimate purpose of the present program is to provide additional knowledge necessary for the prediction of transfer processes in both uniform and non-uniform turbulent flow. It is natural to inquire as to whether relationships derived from uniform flow studies will be useful in the prediction of transport phenomena under conditions of non-uniform flow, and the results of this thesis confirm to some extent the validity of such an approach.

The experimental work at the Institute in the study of uniform turbulent flow with uniform heat transfer has been directed toward the calculation of the eddy conductivity and the eddy viscosity, quantities which are measures of the contribution of the turbulence processes to the transfer of heat and momentum, respectively. These eddy quantities have been defined for uniform turbulent flow by means of the following equations (4), and may be calculated directly

from a knowledge of the point values of temperature, thermal flux, velocity, and shear.

$$\frac{\dot{q}}{c_p \sigma} = -(\epsilon_c + K)\frac{\partial T}{\partial s} \tag{1}$$

$$\frac{\tau}{\rho} = -(\epsilon_m + \nu)\frac{\partial u}{\partial s} \tag{2}$$

An explanation of the symbols used in the above equations and in all succeeding equations is given in the table of nomenclature.

Point values of the eddy conductivity and the eddy viscosity may also be determined for non-uniform flow from a knowledge of the pattern of the temperature and velocity fields. The calculations involve an integration of the following partial differential equations which may be derived from Equations 1 and 2 together with an energy balance and a force balance on the flowing fluid. The velocities, velocity derivatives, and temperature derivatives at a point are regarded as known from the experimental data.

$$\frac{\partial}{\partial x} c_p \sigma (\epsilon_c + K)\frac{\partial T}{\partial x} + \frac{\partial}{\partial y} c_p \sigma (\epsilon_c + K)\frac{\partial T}{\partial y} = c_p \sigma u \frac{\partial T}{\partial x} + c_p \sigma v \frac{\partial T}{\partial y} \tag{3}$$

$$\frac{\partial}{\partial x}\sigma(\epsilon_m + \nu)\frac{\partial u}{\partial x} + \frac{\partial}{\partial y}\sigma(\epsilon_m + \nu)\frac{\partial u}{\partial y} = \sigma u \frac{\partial u}{\partial x} + \sigma v \frac{\partial u}{\partial y} - g\frac{\partial p}{\partial x} \tag{4}$$

The experimental data reported here are concerned with the distributions of temperature and air speed in the wake of a long heated cylinder placed normal to a two-dimensional, turbulently flowing air stream. Measurements were made in vertical traverses at several stations downstream from the cylinder. A study of the temperature and velocity fields yields direct information on the relative rates of heat and momentum transfer in non-uniform flow of this type. Although experimental data are available for the distributions of velocity (5,6,7,8,9,10,11) and temperature (6,7,8,9) in the wake of a cylinder, detailed explorations of the wake far downstream from the midline of a cylinder have not been undertaken, and one purpose of the present experimental program is to provide such data.

Previous to the work reported here, experiments of a similar nature were conducted in this laboratory (12,13). These earlier measurements yielded temperature and air speed distributions in the wake of a relatively large cylinder placed normal to a turbulently flowing air stream in an isothermal channel. Because the diameter of the cylinder was large in comparison with the channel height, measurements taken more than ten diameters downstream strongly reflected the disturbing effects of the channel walls. The distortion of the wake, while not vitiating any results obtained, merely introduced another factor into the study of an already complex phenomenon. In addition the data were chiefly taken in the immediate vicinity of the cylinder, and as such provided information on the shedding

of Kármán vortices (14,15). While an interesting study in itself, such an investigation does not provide any significant information regarding the nature of the transfer occurring in the greater portion of the wake, but belongs instead in the domain of the boundary layer theory (16). It was generally felt that more useful information about the transfer processes could be obtained through a study of the portion of the wake in which similarity is found to exist. Geometrical similarity is said to exist in the wake when the dimensionless velocity distribution, $\frac{u - u_o}{u_c - u_{oc}}$, and the dimensionless temperature distribution, $\frac{T - T_o}{T_c - T_o}$, may each be described in terms of a single parameter. To minimize the effect of the channel walls while still utilizing primarily the same equipment, a smaller cylinder was used for the present investigations.

The integration of Equations 3 and 4, yielding point values of ϵ_c and ϵ_m, should provide all the desired information relating to the transfer of heat and momentum in the cylinder wake. However, the shapes of the experimental profiles in the wake of a cylinder are such that considerable uncertainty results in the calculated values of the eddy conductivity and the eddy viscosity at the center and near the edge of the wake. For this reason, such an approach has not been used in the present investigations. The efforts of the present study have been directed toward the prediction of temperature and velocity distributions from an assumed distribution of the eddy quantities.

It is possible to predict the measured temperature and air

speed distributions with accuracy in the range for which experimental data are available. The most useful correlation is based upon the solution of the following equations

$$\frac{\partial}{\partial Y}(\epsilon_c + K)\frac{\partial T}{\partial Y} = u_{oc}\frac{\partial T}{\partial X} \tag{5}$$

$$\frac{\partial}{\partial Y}(\epsilon_m + \nu)\frac{\partial u_d}{\partial Y} = u_{oc}\frac{\partial u_d}{\partial X} \tag{6}$$

in which it is assumed that the eddy conductivity and the eddy viscosity are constants throughout the region of the wake considered. It is shown that the resulting Gaussian distributions are entirely adequate for the description of the temperature and air speed distributions in that portion of the wake throughout which similarity occurs. The measurements reported here are found all to lie substantially in this region.

Transport phenomena in the plane symmetric wake have been studied for a number of years, and several phenomenological theories of the turbulence processes have grown out of such work (9,17,18,19). These theories are reviewed in some detail with particular reference to their utility and to the degree with which they describe the available data. It is shown that the assumed nature of the turbulence has but little effect upon the resulting calculated temperature and velocity profiles, and hence quantities of greater significance

are the heat flux and momentum transfer normal to the direction of mean flow. These quantities are

$$\frac{\dot{q}_n}{c_p \sigma} = -(\epsilon_t + K)\frac{\partial T}{\partial y} = \overline{v'T'} - K\frac{\partial T}{\partial y} \qquad (7)$$

$$\frac{\tau_n}{\rho} = -(\epsilon_m + \nu)\frac{\partial u}{\partial y} = \overline{v'u'} - \nu\frac{\partial u}{\partial y} \qquad (8)$$

The above terms are primarily responsible for the spreading of the temperature and velocity wakes with distance downstream. Although no direct experimental determinations of the normal heat and momentum flux are presented here, a number of significant conclusions may be drawn from a study of the few such data (9) in the current literature, and of the values calculated from the temperature and air speed distributions reported in this thesis. Point values of heat flux in the wake calculated from the theoretical relations developed compare favorably with values of the normal heat flux determined by integration of Equation 3.

This discussion leads naturally to an investigation of the pertinent work based upon the statistical theory of turbulence (20,21,23). It is indicated that for a full understanding of the transport processes occurring in the wake it is necessary to obtain measurements of the instantaneous fluctuating velocity and temperature

components and their correlations which characterize the local structure of the turbulent field. Available data (9,10,23) of this nature serve to indicate in a semiquantitative fashion the relative rates of heat and momentum transfer as a function of position in the wake.

Data are also reported for the transfer of heat from the surface of the cylinder as a function of stream velocity and average cylinder surface temperature. These data are sufficient for the calculation of gross heat transfer coefficients. A comparison with the data of other investigators (1,24) shows coefficients as much as 50% higher. Good agreement with the data of Mason (13) is obtained. The following equation is proposed for the calculation of overall transfer coefficients throughout the range of flow conditions studied.

$$\frac{h_c d}{k_f} = 1.178 \left(\frac{u_{oc} d \sigma}{\mu_f} \right)^{0.368} \qquad (9)$$

Many engineering design problems involving turbulent transfer are concerned with non-uniform phenomena, and often are of such complexity as to preclude any analytical treatment, even though distributions of eddy conductivities, eddy viscosities, and eddy diffusivities are available. A number of methods for solving such problems have been developed (25,26,27,28). One of the more promising methods employs the electric analog computer (28) which is well adapted to the solution of partial differential equations of the parabolic type.

The Institute analog computer (29) has been used to calculate the non-uniform distribution of temperature in a two-dimensional, turbulently flowing air stream and the results have been found to represent with accuracy available experimental data (30) taken under the same boundary conditions.

Equipment and Experimental Methods

The experimental apparatus used in this investigation has been described elsewhere in detail (31). For the purposes of the present study it may be considered to consist of a wind tunnel, 162 inches long, 12 inches wide, and nominally 0.7 inches in height, and a traversing mechanism for positioning the measuring instruments in the channel. Figures 1, 2, and 3 show the general features of the equipment. The upper and the lower channel walls were of 1/4 inch rolled copper, and served as thermal connections between the air stream and two independently circulating oil baths. A cross-section of the channel and the oil baths constitutes Figure 4. The baths were used to control separately the temperatures of the upper and the lower channel walls throughout the range of from 70 to 130°F. The bakelite blocks which formed the sides of the channel were free to slide, permitting the positioning of the traversing gear mechanism at arbitrary stations downstream from the channel entrance. Figure 5 shows the traversing gear and the method used to support the measuring instruments in the channel.

By means of a variable speed blower, preconditioned air was forced through the conduit. The range of Reynolds numbers available was from 2,000 to 70,000. Static pressures in the channel were measured by means of three piezometer bars (located in the upper copper plate) connected to a bank of kerosene-air manometers. The manometer bank and the cathetometer used in the measurements are shown in Figure 6. Weight rates of flow of air were determined by measurement of the pressure drop across a venturi tube of conventional design. The potentiometers and resistance bridges used in all electrical measurements and the air stream and oil bath monitoring circuits were located in the temperature bench shown in Figure 7.

A 11-3/4 inch section of 0.0318 inch OD stainless steel hypodermic tubing was mounted midway between the walls of the channel 69 inches from the upstream entrance. The tubing itself served as the heating element in the experiments. The cylinder was held transverse to the air stream by means of rigid yokes mounted on the traversing gear ways. The yokes applied tension to two 0.02 inch piano wires silver-soldered into the ends of the tubing. Figure 8 shows the cylinder mounted in the channel and Figure 9 shows one of the yokes.

Potential and current leads were soft-soldered onto the cylinder near the ends and were brought out from each side to a junction box on the yoke (Figure 9). The effective heated length of the cylinder was measured electrically to be 7.93 inches. Current was fed to the cylinder through the circuit shown in Figure 10 and

measurements of the voltage drop across a 1500-75 ohm voltage divider and across an 0.005 ohm series resistor provided the necessary data for the calculation of the energy input to the cylinder. These measurements were made with a Type K-2 Leeds & Northrup potentiometer and with a White potentiometer, respectively. The instruments were located near the right end of the temperature bench shown in Figure 7.

Prior to its installation, the cylinder with electrical leads attached was calibrated as a resistance thermometer at three different temperatures in a well agitated oil bath. Before calibration the cylinder was strained by applying tension equivalent to that expected when mounted in the air stream. At each calibration temperature approximately four hours were allowed for final temperature equilibrium to be attained. Measurements of the resistance of the cylinder were made with a Mueller bridge and the temperature of the bath was similarly determined by measurement with a conventional strain-free platinum resistance thermometer. The energy dissipation in the cylinder during calibration due to the bridge current was 4.5×10^{-4} watts, and this is believed to have introduced an error due to radial temperature gradients of less than $0.06^{\circ}F$. While being calibrated the cylinder was placed in an elongated U section of 10 mm glass tubing to prevent contact between the cylinder and the oil in the bath. This arrangement introduced an error due to conduction to the surroundings which was completely negligible at the highest temperature encountered in the calibration procedure. The cylinder

was also calibrated at 80°F and at 100°F when in place in the channel with tension applied. These data were taken as the limit of the resistance of the cylinder determined as a function of current flowing, as the current was decreased without limit. It was found that the results reproduced the original calibration within the limit of uncertainty of the original measurements. During the course of the experimental program, several additional calibration points were taken as a check with no air flowing and with the channel walls at 100°F. The maximum calibration change noted was 0.5 °F.

Measurements of temperature and air speed were made with a hot wire anemometer which could be positioned at any point in the channel. Details of the use and calibration of this instrument have been described (32,33). The anemometer consisted of a 3/8 inch long, 1/2 mil platinum wire supported between the tips of two needles (Figure 6). Air speeds were measured in the wake by conventional constant resistance anemometry techniques. The hot wire was calibrated at several speeds against an ordinary impact head tube (Figure 6).

Although the single hot wire anemometer is sensitive only to the absolute value of the local air velocity, i.e., the air speed, throughout the region of the wake investigated the difference between the air speed and the horizontal component of the velocity vector was less than 0.1%. For this reason the air speed will be referred to henceforth simply as velocity unless a distinction is desired between vertical and horizontal components of the velocity.

For temperature measurements the wire served as a low heat capacity platinum resistance thermometer. Calibration was made in still air. It was necessary to apply corrections to the observed temperatures in a moving stream to compensate for the effects of isentropic compression of the air stream near the forward stagnation point on the wire. Since in still air the bridge current necessary for resistance measurements caused a heating of the wire and the surrounding air, an additional correction was necessary for measurements made in regions of non-vanishing velocity. These corrections have been discussed at length elsewhere (34).

Velocity and temperature measurements were made in vertical traverses at each of seven distances downstream from the midline of the cylinder for nominal air speeds of 30, 60, and 90 feet per second. For each traverse the air entered at 100°F and the channel walls were maintained at 100°F. Total wattage dissipation from the cylinder was 21.35 watts or 2.692 watts per inch. Two additional traverses were made at a nominal air flow of 30 feet per second with no power dissipation from the cylinder to assist in analyzing the effects of natural convection on the distribution of velocity.

Measurements of the wattage dissipation from the cylinder as a function of cylinder resistance were made at a number of different rates of air flow. The average cylinder temperature was calculated from the measured cylinder resistance and the previously mentioned calibration data. Because of the uneven distribution of temperature throughout a section perpendicular to the axis of the

cylinder, the observed resistance was not simply related to the average cylinder temperature. However, the effect of the uneven distribution of temperature has been shown to affect the heat flux from the cylinder only slightly. The difference between average surface temperature and average bulk temperature of the cylinder was less than 0.15°F. The uncertainty in the calculated values of the heat transfer coefficient for low rates of heat transfer is dependent chiefly upon uncertainties in the temperature calibration of the cylinder itself. Energy input was calculated from the measurement of the voltage drop across two calibrated resistors. Bulk velocities were established on the basis of readings of a venturi meter. Data were taken for five different bulk velocities and included wattage dissipations of from 0.3 to 37.4 watts.

Experimental Results

Velocity calibration data were obtained for the hot wire anemometer at the beginning and at the end of each traverse. It was known that the velocity calibration of the hot wire was not constant, but that it exhibited a systematic variation with operating time (33). This drift was due in part to the accumulation of foreign material on the surface of the wire. It is felt that the use of soft solder in mounting the wire on its needle supports contributed also to the calibration drift through the gradual flow of solder onto the surface of the wire adjacent to the supports.

Calibration data were obtained at three specified reference

velocities, and the information at each calibration velocity was plotted as a function of the operating time of the hot wire. A smooth curve was faired through the points. This procedure made it possible to establish an instantaneous velocity calibration curve for the anemometer, and the reported velocities were determined on this basis. At several times during the course of the experimental program, abrupt shifts in the calibration of the wire were observed. Such irregularities were probably the result of a sudden accumulation on the wire of dust particles, or an accidental "burning off" of the wire. Because of insufficient calibration data at some periods in the history of the anemometer, these calibration shifts were sufficient to cause uncertainties in some of the reported velocities of as much as 4%, although for any given traverse the maximum deviation of the experimental points from the best smooth curve through the points is not more than 1%. The experimental point velocities for each of the flow conditions investigated have been recorded in Table I. To reduce all experimental velocities to the same basis, the point values for each bulk velocity have been adjusted to correspond to the same average weight rate of flow, absolute pressure, channel height, and humidity. These averages were taken as the arithmetic means of the values for each traverse at a given nominal Reynolds number. Several specimen velocity traverses corresponding to a nominal air speed of 30 feet per second are shown in Figure 11. Traverses for nominal air speeds of 60 and 90 feet per second exhibit the same characteristics as do those traverses

displayed in Figure 11. The relatively smooth profiles obtained indicate that the complex region of the wake was not entered. The irregular features observed by Billman (12) and by Mason (13) in the regions close to a cylinder are conspicuously absent from the distributions shown.

A cursory inspection of the time variation of the temperature calibration indicated that the calibration drift was small and that the calibration could be considered to remain stationary with respect to time for a given temperature traverse. Temperature calibration data were obtained at the end of each set of wake measurements at a given bulk Reynolds number, and at the beginning and at the end of each period for which the experimental work was halted for any appreciable amount of time. The temperature data have been recorded in Table I as a function of position in the channel for each of the flow conditions studied. Because of uncertainties regarding the value of the recovery factor for the hot wire, the temperatures entered in Table I have not been corrected for impact effects. Figure 12 contains specimen temperature traverses at a bulk velocity of 30 feet per second. The distributions shown are quite characteristic of the data for all flow conditions. The deviation of the experimental temperatures from the smoothed curves is in general less than $0.03^{\circ}F$ except near the edge of the wake where differences as great as $0.05^{\circ}F$ were noted. It is felt that the hot wire when used as a temperature measuring device could not in general be relied upon for more precise measurements under flow conditions,

especially where large temperature gradients result. Mechanical vibrations have been observed which are sufficient to cause observational errors as great as 0.1°F in extreme gradients because of the variability of the position of the wire.

The results of measurements of wattage dissipation from the cylinder as a function of average cylinder temperature are presented in Table II, and have been utilized to calculate conventional heat transfer coefficients. The heat transfer coefficient for conduction and convection is defined as

$$h_c = \frac{\dot{Q}_c}{\pi d L (T_s - T_o)} \qquad (10)$$

where $\dot{Q}_c$ is the total heat transferred from the cylinder less the heat loss due to radiation. The coefficient as defined in Equation 10 is presented as a function of the flow parameters in Figure 13 which is a plot of the Nusselt number vs the Reynolds number.

The data correlate well with the results of Mason (13) obtained in this laboratory, and substantiate the trend observed by him. At low Reynolds number, heat transfer coefficients as much as 50% above those given by McAdams (1) are found. This difference is probably due to the relatively high level of turbulence which existed in the flow channel used for the present measurements, since it is known that at low Reynolds numbers the effect of the level of turbulence on the heat transfer characteristics of cylinders is large (35).

Furthermore, in a channel whose height was only an order of magnitude greater than the cylinder diameter, a relatively small value of the length parameter characterizing the local turbulence scale would be expected. A scale comparable with the dimensions of the cylinder could be expected to produce anomalous heat transfer effects. It is suggested that wattage dissipation data be obtained under circumstances similar to those encountered in the experimental work reported here, and that a systematic study be made of the influence of the structure of the turbulent field on the overall heat transfer characteristics of cylinders.

In view of the uncertainties associated with the interpretation of the hot wire calibration data, the overall accuracy claimed for the reported velocities is not high. Absolute errors of as much as 4% are expected for some of the traverses. Measurements were confined to downstream distances greater than 15 cylinder diameters. Any errors due to the slow time response of the hot wire are negligible, since in this region of the wake the complex behavior associated with the shedding of Kármán vortices (14, 15) was absent.

In general, velocity measurements made in the immediate vicinity of a solid boundary are in error because of increased heat conduction from the wire. However, none of the present data are subject to this uncertainty, all experimental measurements having been obtained in the center region of the flow channel at relatively large distances from the heated cylinder.

Mason (30) has previously analyzed the accuracy of the hot wire

as a temperature measuring device under conditions similar to those encountered in the present experimental work, and reports a maximum root mean square error of 0.14°F. The experimental work reported here indicates a precision of measurement between 0.03 and 0.05°F, the latter value being encountered near the edge of the wake.

Because the temperature data have been correlated in terms of a rise above measured free stream temperature for each traverse, the precision of the measurements is more significant than their accuracy in the analysis of the present data.

The resistance calibration of the cylinder as a function of its average temperature was found to be linear to within 0.5°F over the range 80 to 250°F. A least squares line was fitted to the data, and it is felt that the reported temperatures are correct to within ± 0.3°F.

Throughout all of the experimental work in which energy was being dissipated from the cylinder, the power was maintained within 0.1% of the prescribed value. The wattage dissipation was known to within 0.1%.

The error in the positioning of the hot wire with respect to the boundaries of the channel did not exceed 0.002 inches. Since the temperature and velocity gradients encountered in this experimental work were not extreme, this position uncertainty did not inject any noticeable error into the measurements. In the case of temperature measurements the maximum possible error which could be ascribed to this cause was 0.1°F. The greatest possible uncertainty

introduced into the interpretation of the velocity measurements as a result of errors in the position of the anemometer in the channel is less than 1%. The maximum uncertainty in the reported value of the X coordinate for each traverse is 0.01 inch.

Theory

The analytical problem of establishing the transfer of heat and momentum in the wake of a heated cylinder has been previously attacked, and several reasonably successful methods of prediction of temperature and velocity fields are available (9,17,18,19). Most of these correlations are based upon phenomenological considerations of the turbulence processes, yet they have been found to represent adequately the distributions of temperature and velocity in the cylinder wake. The following discussion serves to review the general principles involved in the derivation of such correlations, and presents some results which have been found useful in analyzing the data presented in this thesis.

Since it has been found practical to describe the temperature and velocity fields independently of one another the following treatment has been arranged to allow independent discussions of the hydrodynamic problem and of the problem of prediction of temperatures and of thermal flux under the substantially non-uniform flow conditions which are known to prevail in the wake of the cylinder.

Osborne Reynolds (36) observed in 1883 that in any fluid which was caused to flow at a velocity exceeding some critical value,

depending upon the properties of the fluid and upon the geometrical constraints imposed on the flow, there were manifest in the fluid certain irregular motions of a scale less than that of the normal hydrodynamic motion described by the Navier-Stokes (37) equations. These irregular motions were entirely random in nature and had the effect of increasing the transport of momentum and of any other transferrable quantity such as heat or matter. This increased transfer was the result of the gross movement of eddies of fluid within the stream resulting from instantaneous fluctuations in the local structure of the flow field. Since engineering flow problems are often concerned with such states of turbulent fluid motion, rather than with laminar fluid flow in which properties are transferred solely by the mechanisms of molecular conduction, diffusion, etc., the properties of motion of the former type are of great importance.

The Navier-Stokes equations have been found to represent satisfactorily the experimentally observed laminar motion of fluids under a considerable variety of boundary conditions. In rectangular cartesian coordinates these equations become, for an incompressible fluid (37),

$$\frac{\partial u}{\partial \theta} + u\frac{\partial u}{\partial x} + v\frac{\partial u}{\partial y} + w\frac{\partial u}{\partial z} = X - \frac{1}{\rho}\frac{\partial p}{\partial x} + \nu\left(\frac{\partial^2 u}{\partial x^2} + \frac{\partial^2 u}{\partial y^2} + \frac{\partial^2 u}{\partial z^2}\right) \quad (11)$$

$$\frac{\partial v}{\partial \theta} + u\frac{\partial v}{\partial x} + v\frac{\partial v}{\partial y} + w\frac{\partial v}{\partial z} = Y - \frac{1}{\rho}\frac{\partial p}{\partial y} + \nu\left(\frac{\partial^2 v}{\partial x^2} + \frac{\partial^2 v}{\partial y^2} + \frac{\partial^2 v}{\partial z^2}\right) \quad (12)$$

$$\frac{\partial w}{\partial \theta} + u\frac{\partial w}{\partial x} + v\frac{\partial w}{\partial y} + w\frac{\partial w}{\partial z} = Z - \frac{1}{\rho}\frac{\partial p}{\partial z} + \nu\left(\frac{\partial^2 w}{\partial x^2} + \frac{\partial^2 w}{\partial y^2} + \frac{\partial^2 w}{\partial z^2}\right) \quad (13)$$

The conservation of matter throughout the flow field is expressed analytically by the equation of continuity (37).

$$\frac{\partial \rho}{\partial \theta} + \rho \left(\frac{\partial \mathcal{U}}{\partial x} + \frac{\partial \mathcal{V}}{\partial y} + \frac{\partial \mathcal{W}}{\partial z} \right) = 0 \qquad (14)$$

Although strictly speaking, the present experimental work concerns the flow of air, which is a compressible fluid, it can be readily shown that for speeds much less than the local velocity of sound and for small temperature differences, little error is introduced through the assumption of incompressibility. Throughout the following discussion all compressibility effects will be entirely neglected.

In a turbulent field, if the flow is steady, each of the components of velocity may be conveniently resolved into the sum of two terms. The first term is taken to be the mean value of the velocity component at a point, i.e., the average taken over a period of time which is long in comparison with the period of fluctuations in the velocity. The second term then represents the instantaneous fluctuating characteristics of the velocity component, and has a time average of zero. Thus, into Equations 11, 12, 13, and 14 are introduced

$$\mathcal{U} = u + u' \qquad (15)$$

$$\mathcal{V} = v + v' \qquad (16)$$

$$\mathcal{W} = w + w' \qquad (17)$$

where

$$\frac{1}{\Delta\theta}\int_{\theta}^{\theta+\Delta\theta} u'\,d\xi = \frac{1}{\Delta\theta}\int_{\theta}^{\theta+\Delta\theta} v'\,d\xi = \frac{1}{\Delta\theta}\int_{\theta}^{\theta+\Delta\theta} w'\,d\xi = 0 \qquad (18)$$

If Equations 11, 12, 13, and 14 are combined and averaged over a period of time which is long in comparison to the period of random velocity fluctuations, yet still short in comparison to the time required for measurement there is obtained for steady flow the set of equations

$$u\frac{\partial u}{\partial x} + v\frac{\partial u}{\partial y} + w\frac{\partial u}{\partial z} =$$

$$X - \frac{1}{\rho}\frac{\partial p}{\partial x} + \frac{\partial}{\partial x}\left(\nu\frac{\partial u}{\partial x} - \overline{u'u'}\right) + \frac{\partial}{\partial y}\left(\nu\frac{\partial u}{\partial y} - \overline{u'v'}\right) + \frac{\partial}{\partial z}\left(\nu\frac{\partial u}{\partial z} - \overline{u'w'}\right) \qquad (19)$$

$$u\frac{\partial v}{\partial x} + v\frac{\partial v}{\partial y} + w\frac{\partial v}{\partial z} =$$

$$Y - \frac{1}{\rho}\frac{\partial p}{\partial y} + \frac{\partial}{\partial x}\left(\nu\frac{\partial v}{\partial x} - \overline{u'v'}\right) + \frac{\partial}{\partial y}\left(\nu\frac{\partial v}{\partial y} - \overline{v'v'}\right) + \frac{\partial}{\partial z}\left(\nu\frac{\partial v}{\partial z} - \overline{v'w'}\right) \qquad (20)$$

$$u\frac{\partial w}{\partial x} + v\frac{\partial w}{\partial y} + w\frac{\partial w}{\partial z} =$$

$$Z - \frac{1}{\rho}\frac{\partial p}{\partial z} + \frac{\partial}{\partial x}\left(\nu\frac{\partial w}{\partial x} - \overline{u'w'}\right) + \frac{\partial}{\partial y}\left(\nu\frac{\partial w}{\partial y} - \overline{v'w'}\right) + \frac{\partial}{\partial z}\left(\nu\frac{\partial w}{\partial z} - \overline{w'w'}\right) \qquad (21)$$

For steady flow the continuity equation becomes

$$\frac{\partial u}{\partial X} + \frac{\partial v}{\partial Y} + \frac{\partial w}{\partial Z} = 0 \qquad (22)$$

Reynolds interpreted the terms $\overline{u'u'}$, $\overline{u'v'}$, $\overline{u'w'}$, $\overline{v'u'}$, $\overline{v'v'}$, $\overline{v'w'}$, $\overline{w'u'}$, $\overline{w'v'}$, and $\overline{w'w'}$ as turbulent shearing stresses, and if they are so identified, Equations 19, 20, and 21 are found to assume a form similar to that of Equations 11, 12 and 13. Of course, for any given set of boundary conditions in a turbulent flow regime, the turbulent shearing stresses still remain unknown. The efforts of experimental and theoretical investigators have been directed toward the solution of the above equations with varying degrees of success.

Equations 19, 20, 21, and 22 may be applied to the analysis of the wake behind a cylinder whose center is at the origin of a rectangular coordinate system. The X axis proceeds in the direction of main flow of the stream, the Y axis perpendicular to the plane of the wake, and the Z axis parallel to the axis of the cylinder which is assumed to be infinitely long (Figure 14). For the two dimensional, steady case in which there are no forces Equations 19, 20, 21 and 22 reduce to

$$u\frac{\partial u}{\partial x} + v\frac{\partial u}{\partial y} = -\frac{1}{\rho}\frac{\partial p}{\partial x} + \frac{\partial}{\partial x}\left(\epsilon_{m_{xx}} + \nu\right)\frac{\partial u}{\partial x} + \frac{\partial}{\partial y}\left(\epsilon_{m_{xy}} + \nu\right)\frac{\partial u}{\partial y} \qquad (23)$$

$$u\frac{\partial v}{\partial x} + v\frac{\partial v}{\partial y} = -\frac{1}{\rho}\frac{\partial p}{\partial y} + \frac{\partial}{\partial x}\left(\epsilon_{m_{yx}} + \nu\right)\frac{\partial v}{\partial x} + \frac{\partial}{\partial y}\left(\epsilon_{m_{yy}} + \nu\right)\frac{\partial v}{\partial y} \qquad (24)$$

$$\frac{\partial u}{\partial x} + \frac{\partial v}{\partial y} = 0 \qquad (25)$$

where in analogy to the expressions for laminar shearing stresses, the turbulent stresses have been replaced by expressions containing the eddy viscosity, bringing into evidence the contribution of the turbulence processes to the transfer of momentum in the stream.

$$-\overline{u'u'} = \epsilon_{m_{xx}}\left(2\frac{\partial u}{\partial x}\right) \tag{26}$$

$$-\overline{u'v'} = \epsilon_{m_{xy}}\left(\frac{\partial u}{\partial y} + \frac{\partial v}{\partial x}\right) \tag{27}$$

$$-\overline{v'u'} = \epsilon_{m_{yx}}\left(\frac{\partial v}{\partial x} + \frac{\partial u}{\partial y}\right) \tag{28}$$

$$-\overline{v'v'} = \epsilon_{m_{yy}}\left(2\frac{\partial v}{\partial y}\right) \tag{29}$$

Several solutions to the above equations have been obtained for laminar flow where all the components of the eddy viscosity are zero (37). Because of the non-linearity of Equations 23 and 24, no exact solution exists which describes the entire flow region downstream from a cylinder.

These equations may be linearized by the approximate methods of the boundary layer theory (16). It is assumed that $U = u - u_{oc}$ and v are small, and for a first approximation, all terms which are quadratic in the velocities and velocity derivatives are neglected. With this condition it can be shown that a single equation results.

$$u_{oc}\frac{\partial u}{\partial x} = -\frac{1}{\rho}\frac{\partial p}{\partial x} + \frac{\partial}{\partial y}\left(\epsilon_{m_{xy}} + \nu\right)\frac{\partial u}{\partial y} \tag{30}$$

For the purposes of comparison with the experimental data it is convenient to remove the pressure gradient term from the above equation. In the apparatus used the free channel flow may be represented approximately by

$$\frac{d}{dY}\left(\epsilon_{m_{XY}} + \nu\right)\frac{du_o}{dY} = \frac{1}{\rho}\frac{\partial p}{\partial X} \tag{31}$$

where u_o is a function of Y alone. This description is reasonably valid in the center region of the channel even when $\epsilon_{m_{XY}}$ is assumed constant. If the velocity deficiency is defined as

$$u_d = u_o - u \tag{32}$$

a combination of this definition with Equations 30 and 31 yields the following expression. It will be assumed throughout the ensuing discussion that the turbulence may be considered isotropic in the sense that all the components of the eddy viscosity tensor will be regarded as identical. With this assumption the directional subscripts will be dropped.

$$u_{oc}\frac{\partial u_d}{\partial X} = \frac{\partial}{\partial Y}\left(\epsilon_m + \nu\right)\frac{\partial u_d}{\partial Y} \tag{33}$$

The above equation has proved to be one of the most convenient starting points for the development of the phenomenological theories of motion in the wake of a cylinder, though analyses based upon statistical theories of turbulence employ Equations 19 and 20 and additional relationships between the correlation coefficients.

The present data have been found to correlate well with the solution of Equation 33 under the assumption that ϵ_m remains constant throughout the wake. The solution of Equation 33 for a line disturbance in an infinite stream of fluid is (38)

$$u_d = u_o - u = \frac{u_{oc}}{2\sqrt{\pi}} \sqrt{\frac{u_{oc}\, d}{\epsilon_m + \nu}} \sqrt{\frac{d}{x}}\; e^{-\frac{u_{oc}\, d}{\epsilon_m + \nu} \frac{(y/d)^2}{4(x/d)}} \qquad (34)$$

The above expression should describe reasonably well the distribution of the deficiency velocity for downstream distances large in comparison to the cylinder diameter.

Letting $y = 0$ in Equation 34 there is obtained the expression

$$u_{oc} - u_c = \frac{u_{oc}}{2\sqrt{\pi}} \sqrt{\frac{u_{oc}\, d}{\epsilon_m + \nu}} \sqrt{\frac{d}{x}} \qquad (35)$$

which indicates a linear relationship between the centerline deficiency velocity and $\sqrt{\frac{d}{x}}$. In Figure 15 the ratio $\frac{u_{oc} - u_c}{u_{oc}}$ is shown as a function of $\sqrt{\frac{d}{x}}$ for all the traverses reported. The linear relationship indicated in Equation 35 is seen to be experimentally verified. On the basis of the expression shown above the slope of the curve of Figure 15 is numerically equal to $\frac{1}{2\sqrt{\pi}} \sqrt{\frac{u_{oc}\, d}{\epsilon_m + \nu}}$ and appears to be substantially independent of u_{oc} . From the slope of the curve, the value of $\frac{u_{oc}\, d}{\epsilon_m + \nu}$ is calculated to be 13.3.

It is convenient at this point to associate with the wake, at any given distance downstream, a characteristic width. This

characteristic width will be defined, for any specified distance downstream as that value of Y at which $u_o - u$ reaches half its maximum value, $u_{oc} - u_c$. Figure 16 indicates schematically the method of identification of this width. The above definition when applied to Equation 34 yields the following dimensionless expression for the characteristic width of the velocity wake

$$\frac{Y_u}{d} = \sqrt{4 \ln 2} \sqrt{\frac{\epsilon_m + \nu}{u_{oc} d}} \sqrt{\frac{x}{d}} \qquad (36)$$

The experimental values of $\frac{Y_u}{d}$ are presented in Figure 17 as a function of the square root of the distance downstream from the centerline of the cylinder. Agreement with the predicted relationship of Equation 36 is good. The value of $\frac{u_{oc} d}{\epsilon_m + \nu}$ determined from Figure 17 is 37.8. No explanation has been found for the discrepancy in the two values of the "turbulent Reynolds number" although it is felt that neglect of transverse velocity components in the analysis of the wake may have contributed significantly to the disagreement noted.

Upon combination of Equations 34, 35, and 36 there results the universal dimensionless velocity distribution,

$$\frac{u - u_o}{u_c - u_{oc}} = e^{-\left(\frac{Y}{Y_u}\right)^2 \ln 2} \qquad (37)$$

which may be used to establish the velocity at any point in the wake when y_u and $u_c - u_{oc}$ are known as functions of X. In Figure 18 are presented in dimensionless form all the experimental velocity data of the present investigation. It is noteworthy that values obtained at all three bulk velocities are correlated by the same theoretical equation. The agreement with the predicted relationship of Equation 37 is considered quite satisfactory. The data of Figure 18 represent measurements taken at seven different downstream distances for each of the three bulk air speeds. It should be emphasized that the scatter of the points shown is a result of the comparison of the data of several traverses. The data for any given traverse define a relatively smooth curve (Figure 11). The deviations from the theoretical curve encountered for values of $\frac{y}{y_u} > 1.5$ indicate the effect of the channel walls in disturbing the flow from the idealized condition assumed. The standard deviation of the points shown from the smooth curve is 0.030.

The equation describing the distribution of temperature due to conduction and convection of heat in a laminar, two-dimensional flow is (24)

$$\frac{\partial}{\partial x}\left(K \frac{\partial T}{\partial x}\right) + \frac{\partial}{\partial y}\left(K \frac{\partial T}{\partial y}\right) = u \frac{\partial T}{\partial x} + v \frac{\partial T}{\partial y} \qquad (38)$$

This relationship may be generalized to apply to distributions in a turbulent field by introducing the instantaneous fluctuating velocity and temperature terms. T is resolved into the sum of

a time average and a fluctuating component

$$T' = T + \tau' \tag{39}$$

where

$$\frac{1}{\Delta\theta} \int_{\theta}^{\theta+\Delta\theta} \tau' \, d\xi = 0 \tag{40}$$

If u and v are replaced by the expressions of Equations 15 and 16, Equation 38 may be combined with Equation 39 to yield

$$\frac{\partial}{\partial x}\left(K \frac{\partial T}{\partial x}\right) + \frac{\partial}{\partial y}\left(K \frac{\partial T}{\partial y}\right) + \frac{\partial}{\partial x}\left(K \frac{\partial \tau'}{\partial x}\right) + \frac{\partial}{\partial y}\left(K \frac{\partial \tau'}{\partial y}\right) =$$

$$(u+u')\frac{\partial}{\partial x}(T+\tau') + (v+v')\frac{\partial}{\partial y}(T+\tau') \tag{41}$$

The time average of this equation becomes

$$\frac{\partial}{\partial x}\left(-\overline{u'\tau'} + K\frac{\partial T}{\partial x}\right) + \frac{\partial}{\partial y}\left(-\overline{v'\tau'} + K\frac{\partial T}{\partial y}\right) = u\frac{\partial T}{\partial x} + v\frac{\partial T}{\partial y} \tag{42}$$

which is seen to be similar to Equation 38 upon identification of $\overline{u'\tau'}$ and $\overline{v'\tau'}$ as additional turbulent heat flux terms.

In the following discussion this analogy will be recognized and, in fact, the turbulent heat transport terms will be replaced by equivalent expressions involving the eddy conductivity, which

expresses the effect of the turbulence in increasing the transport of heat.

$$-\overline{u'T'} = \epsilon_{c_x} \frac{\partial T}{\partial x} \tag{43}$$

$$-\overline{v'T'} = \epsilon_{c_y} \frac{\partial T}{\partial y} \tag{44}$$

Equations 43 and 44 may be regarded as alternative definitions of the eddy conductivity (4). In the discussion which follows the turbulent field will be assumed to be everywhere isotropic so that all components of the eddy conductivity will be identical. Equation 42 now assumes the familiar form

$$\frac{\partial}{\partial x}(\epsilon_c + K)\frac{\partial T}{\partial x} + \frac{\partial}{\partial y}(\epsilon_c + K)\frac{\partial T}{\partial y} = u\frac{\partial T}{\partial x} + v\frac{\partial T}{\partial y} \tag{45}$$

For a description of the temperature distribution in the wake of a heated cylinder it has been found possible to represent satisfactorily the data of this thesis by the solution of the above relationship under the assumption that conduction downstream and convention normal to the direction of the mean flow may be neglected. If u is replaced by the constant u_{oc} and, furthermore, if ϵ_c is assumed to remain constant throughout the wake, Equation 45 becomes

$$(\epsilon_c + K)\frac{\partial^2 T}{\partial y^2} = u_{oc}\frac{\partial T}{\partial x} \tag{46}$$

The solution of the above equation for a line source of heat in a stream of infinite extent is (38)

$$T - T_0 = \frac{\dot{Q}_c}{2\sqrt{\pi}\, C_p \sigma\, u_{oc} d L} \sqrt{\frac{u_{oc} d}{\epsilon_t + K}} \sqrt{\frac{d}{x}}\, e^{-\frac{u_{oc} d}{\epsilon_t + K} \frac{(y/d)^2}{4 x/d}} \tag{47}$$

Equation 47 is seen to be of the same form as Equation 34 for the deficiency velocity distribution downstream from the cylinder.

The expression for the centerline temperature is obtained by setting $y = 0$. The result is

$$T - T_0 = \frac{\dot{Q}_c}{2\sqrt{\pi}\, C_p \sigma\, u_{oc} d L} \sqrt{\frac{u_{oc} d}{\epsilon_t + K}} \sqrt{\frac{d}{x}} \tag{48}$$

Figure 19 is a plot of $(T_c - T_0) u_{oc}$ as a function of $\sqrt{\frac{d}{x}}$, including data taken at three different air speeds, and indicates the validity of the linear relationship predicted by the above equation. The slope of the line through the points yields the value $\frac{u_{oc} d}{\epsilon_t + K} = 15.6$, which appears to be independent of the nominal Reynolds number of the flow.

If a characteristic width describing the temperature wake is now defined as that value of y at which the temperature difference is one half its maximum value (Figure 16), then upon combination of this definition with Equations 47 and 48, the following relationship results:

$$\frac{y_T}{d} = \sqrt{4 \ln 2} \sqrt{\frac{\epsilon + K}{u_{oc} d}} \sqrt{\frac{x}{d}} \tag{49}$$

If experimentally determined values of y_T/d are plotted as a function of $\sqrt{\frac{x}{d}}$, Equation 49 may be utilized to establish the value of the turbulent Péclet number, $\frac{u_{oc} d}{\epsilon_c + K}$. Such a plot is shown in Figure 17 from which it is seen that the predicted linear dependence of y_T/d upon $\sqrt{\frac{x}{d}}$ does indeed exist. The value of $\frac{u_{oc} d}{\epsilon_c + K}$ obtained from Figure 17 is 15.5. It is felt that the agreement between the two values obtained for the turbulent Péclet number serves to indicate that the above derived equations satisfactorily describe the physical phenomena which occur in the cylinder wake.

Schubauer (39) has presented a correlation between the intensity of isotropic turbulence and the average value of the eddy conductivity. The method of correlation depends upon a measurement of the divergence of the temperature wake behind a heated wire of small diameter. The data of this thesis have been analyzed by the method of Schubauer in order to establish the effective intensity of turbulence in the wake. The value obtained is 3.8% which compares favorably with the value of the free channel intensity obtained by measurement with a compensated hot wire anemometer and circuit of conventional design.

The value of the ratio $\frac{\epsilon_c + K}{u_{oc}}$ was found to be only 15% higher than the average value obtained for the undisturbed channel flow. It appears that for small disturbances in the flowing stream the values of ϵ_c obtained from uniform flow studies may be used with the appropriate partial differential equation and boundary conditions to establish temperature and heat flux distributions under non-uniform conditions of transfer.

A dimensionless, universal temperature distribution may be derived from a combination of Equations 47, 48, and 49. The result is

$$\frac{T - T_o}{T_c - T_o} = e^{-\left(\frac{Y}{Y_T}\right)^2 \ln 2} \tag{50}$$

which is seen to be identical in form with the universal velocity distribution of Equation 37, differing only in the introduction of the appropriate characteristic width for the temperature wake. All the experimental temperature data of this thesis are presented in dimensionless form in Figure 20, and are compared with the above predicted relationship. Although the agreement is good the deviation of the points from the theoretical curve is greater in this case than with the velocity correlation. The data of Figure 20 represent traverses at seven downstream positions, and the scatter of the points represented is again the result of the comparison of data for several traverses. The distributions shown in Figure 12 are characteristic of the smooth individual profiles obtained. It is seen that there is no significant dependence of the distributions upon the bulk Reynolds number of the flow. The standard deviation of the points from the curve is 0.036.

The general method of analysis outlined in the preceding paragraphs has been extended to the correlation of temperature data obtained in the wake of a large heated sphere (40) and in the wake of a large heated cylinder (13). Both experimental investigations

were performed with the same apparatus used in the present experimental work. A similar analysis has been applied to the prediction of concentration distributions in a turbulent diffusion flame apparatus (41) under non-burning conditions of flow. The detailed derivations of the following results differ from those of the preceding analysis only by the introduction of additional terms necessary to account for the increased symmetry.

The expression used to establish the temperature distribution in the wake of a sphere is

$$T - T_o = \frac{\dot{Q}_s}{4\pi \zeta_p \sigma u_{oc} d_s^2} \left(\frac{u_{oc} d_s}{\epsilon_c + K}\right)\left(\frac{d_s}{x - x_o}\right) e^{-\frac{u_{oc} d_s}{\epsilon_c + K} \frac{(y/d_s)^2 + (z/d_s)^2}{4 \frac{x - x_o'}{d_s}}} \qquad (51)$$

where allowance has been made for the existence of a virtual center which differs from the true center of the sphere. The constant x_o/d_s has been determined to be -0.378. It has been found necessary to give the constant x_o'/d_s the different value + 0.40.

Equation 51 contains the assumption that ϵ_c and u remain effectively constant throughout the wake, that conduction in the downstream direction and convection normal to the flow may be neglected, and that the sphere is small and is placed in a fluid stream of infinite extent. It is clearly recognized that these assumptions are quite restrictive, and the degree to which they describe the actual conditions existing is open to question. Nevertheless the results of the analysis have been found to represent the available

experimental data remarkably well.

If the temperature rise along the X axis is denoted by $T_c - T_o$, the following expression may be derived from Equation 51.

$$T_c - T_o = \frac{\dot{Q}_s}{4\pi C_p \sigma U_{oc} d_s^2} \left(\frac{U_{oc} d_s}{\epsilon_c + k}\right) \left(\frac{d_s}{x - x_o}\right) \qquad (52)$$

Experimental data are available (40) for the temperature rise downstream from a heated sphere of large diameter (0.5 inches) placed in a turbulent air stream. The smoothed values of $T_c - T_o$ obtained from the data have been plotted in Figure 21 on the basis of the relationship expressed by Equation 52. The data substantiate the predicted linear relationship between $T_c - T_o$ and $\frac{d_s}{x - x_o}$. The turbulent Péclet number calculated on the basis of the above value for the total conductivity is $\frac{U_{oc} d_s}{\epsilon_c + k} = 22.8$.

From Equation 51 it is possible to find a maximum value of $T - T_o$ for a vertical traverse at any given value of x and z. The corresponding value of $T_m - T_o$ occurs at $Y = 0$ and from Equation 51 is found to have the form

$$T_m - T_o = (T_c - T_o)\, e^{-\frac{U_{oc} d_s}{\epsilon_c + k} \frac{(z/d_s)^2}{4\frac{x - x_o'}{d_s}}} \qquad (53)$$

The characteristic width, Y_T, for the wake is chosen as that value of Y for which $T - T_o = \frac{1}{2}(T_m - T_o)$ in a vertical traverse at a given value of z. This definition results in the following analytical expression, which has the same form for all

values of z .

$$\frac{Y_T}{d_s} = \sqrt{4 \ln 2} \sqrt{\frac{\epsilon_c + K}{u_{oc} d_s}} \sqrt{\frac{x - x_o'}{d_s}} \qquad (54)$$

In Figure 22 values of Y_T/d_s determined from the experimental data have been plotted as a function of $\frac{x - x_o'}{d_s}$. The constant x_o'/d_s has the value 0.40, and it should be noted that this does not yield the same virtual origin that was observed to exist with respect to centerline temperature variation. Such discrepancies merely serve to indicate more strongly certain inadequacies of the correlations presented here. The points shown represent values of Y_T/d_s determined at several different values of z and show a large amount of scatter. It is to be expected that the correlation predicted by Equation 54 would be poor, because the relationship is derived on the basis of a point source of heat, rather than on the basis of a disturbance of finite size. The straight line shown was plotted on the basis of a Péclet number of 22.8 (obtained from Figure 22) and is seen to follow reasonably well the distribution of the points shown.

If Equations 51, 52, 53, and 54 are combined, a universal, dimensionless correlation for the point values of temperature is obtained.

$$\frac{T - T_o}{T_m - T_o} = e^{-\left(\frac{Y}{Y_T}\right)^2 \ln 2} \qquad (55)$$

The above equation is identical with Equation 50 which expresses the variation of the temperature ratio in the wake of a heated cylinder.

The experimental data of eight traverses downstream from a heated sphere are presented in dimensionless form and are compared in Figure 23 with Equation 55. The agreement with the theoretical distribution is striking, and illustrates the degree to which point values of temperature may be estimated under conditions in which the assumptions necessary to the calculation are known to be very poor.

Data are also available for the distributions of temperature and velocity in the wake of a relatively large cylinder (13) placed in the same channel that was used for the experimental work of this thesis. If the additional disturbances introduced by the larger diameter (0.19 inches) of the cylinder are ignored the data may be analyzed with the aid of Equations 48, 49, and 50.

Figure 24 shows a plot of the centerline temperature rise downstream from the cylinder as a function of downstream distance, where the constant x_o/d_c has the value $+1.05$. The data correlate well with the relationship of Equation 48. The slope of the curve of Figure 24 yields a value of the turbulent Péclet number of 20.1 which is in fair agreement with the value obtained for the wake of the sphere, whereas the value of 15.5 in the wake of a small cylinder was approximately three fourths this value. It is suggested that further experimental work be undertaken to investigate the dependence of $\frac{u_{oc}\, d}{\epsilon_c + K}$ upon the size and shape of obstacle placed in a stream. The results presented here are not sufficient for the

formation of any generalization.

The correlation of the wake characteristic widths based upon the relation of Equation 49 is shown in Figure 25 which contains data of eleven traverses and represents measurements made at four different bulk velocities. A straight line expressing the relationship given in Equation 49 has been included. The slope of the line corresponds to a value of 20.1 for the ratio $\frac{U_{oc}\, d_t}{\varepsilon_c + K}$ (determined from Figure 24) and it is seen that within the limits of scatter of the experimental points the theoretical relation is essentially satisfied.

The experimental data of five temperature traverses have been presented in dimensionless form in Figure 26 for comparison with the theoretical expression of Equation 50. Representation of the points by the theoretical curve is considered quite satisfactory, in spite of the relatively large diameter of the cylinder.

Relationships have also been derived for the concentration of natural gas as a function of position downstream from the outlet of a gas tube enclosed in, and concentric with, a larger pipe. A photograph of a section of the apparatus with the outer pipe removed constitutes Figure 27. The equipment was used to study the diffusion of natural gas components into a turbulent air stream as a function of the parameters of flow, both for burning (42) and non-burning (41) conditions. Only the non-burning conditions have been investigated here. The experimental data contain the results of measurements of the mole fraction of natural gas as a function of

position in the larger conduit. Measurements were made at bulk velocities of 25, 50, and 100 feet per second.

By a method analogous to the methods used for the correlation of the sphere and cylinder data, the following relations may be readily derived:

$$\underline{u} = \frac{\underline{u}_o}{16}\left(\frac{u_{oc}\, d_J}{\epsilon_D + D}\right)\left(\frac{d_J}{x - x_o}\right) e^{-\frac{u_{oc}\, d_J}{\epsilon_D + D}\, 4\, \frac{(r/d_J)^2}{\frac{x - x_o'}{d_J}}} \tag{56}$$

$$\underline{u}_m = \frac{\underline{u}_o}{16}\left(\frac{u_{oc}\, d_J}{\epsilon_D + D}\right)\left(\frac{d_J}{x - x_o}\right) \tag{57}$$

$$\frac{R_c}{d_J} = \sqrt{4 \ln 2}\sqrt{\frac{\epsilon_D + D}{u_{oc}\, d_J}}\sqrt{\frac{x - x_o'}{d_J}} \tag{58}$$

$$\frac{C - C_o}{C_m - C_o} = \frac{\underline{u}}{\underline{u}_m} = e^{-\left(\frac{r}{R_c}\right)^2 \ln 2} \tag{59}$$

Figure 28 shows the experimental data for three different bulk velocities plotted on the basis of the relationship indicated in Equation 57. The effects of gravity resulting from differences in density between the air and the natural gas were sufficient to cause the maximum concentration at a given distance downstream to rise

above the centerline of the conduit. The theoretical analysis does not take into account such phenomena, and accordingly the values of η_m plotted in Figure 28 refer to the actual maximum concentration for each traverse rather than to the concentration at the centerline of the conduit. With these corrections the predicted dependence is substantiated. The turbulent diffusion number, $\frac{u_{oc}\, d_J}{\epsilon_D + D}$, is found to vary slightly with velocity as may be seen from the plot. The value at 25 feet per second is $\frac{u_{oc}\, d_J}{\epsilon_D + D} = 400$, which is considerably higher than the value for $\frac{u_{oc}\, d}{\epsilon_c + K}$ found downstream from a symmetrical obstacle in a turbulent stream (see page 35). However, it is to be noted that the method of introduction of the diffusing gas components into the stream differs considerably from the manner in which heat was introduced into a stream by the heated shapes considered. The values of $\frac{u_{oc}\, d_J}{\epsilon_D + D}$ at 50 and 100 feet per second are 435 and 578, respectively. It is noteworthy that the position of the virtual origin varies with velocity (Figure 28). This variation is probably a result of the complex hydrodynamic conditions existing at the point of gas injection. The values of x_o/d_J are considerably greater than those observed for the sphere and for the large cylinder.

The characteristic width of the concentration wake has been presented in Figure 29 as a function of distance downstream from the exit of the natural gas injection tube. Equation 58 indicates a linear relation between the variables R_c/d_J and $\sqrt{\frac{x - x_o'}{d_J}}$. The straight line was plotted for the value $\frac{u_{oc}\, d_J}{\epsilon_D + D} = 400$. Here the disagreement between theory and experiment is more striking. It should

be noted, however, that in the case of the jet of natural gas, at the jet opening, the value of $\mathcal{R}_c$ is necessarily not zero, but perhaps more likely equal to $0.5\,\alpha_J$. As the gas diffuses outward, air diffuses inward and the tendency is for $\mathcal{R}_c$ to remain substantially constant for some time. Thus, analysis based upon the assumption of a jet of non-zero dimensions, rather than on the present assumption of a point source, would be expected to correlate these data.

Experimental data from a total of twenty-seven traverses for the three bulk velocities are presented in Figure 30. The dimensionless method of presentation has been utilized to facilitate comparison with the theory. The predicted distribution of Equation 59 is indicated by the solid curve. The effects of convection due to density differences caused some asymmetry in the concentration profiles. However, by the use of different values of $\mathcal{R}_c$ for each half of a traverse the experimental points are found to correlate well with the expression of Equation 59, with the exception of the points taken 3.25 diameters downstream from the point of injection. These data show a marked deviation from the curve (Figure 30) as would be expected since the assumption of a point source obviously fails for x/d_J of the order of unity.

There is a definite trend to the experimental distributions in that they approach more closely to the theoretical curve with increasing distance downstream, indicating the desirability of a more accurate expression replacing Equation 59. Such a correlation is available (41) but it does not have the advantage of simplicity offered by Equation 59.

Comparison With Other Correlations

Analytical studies of the distributions of velocity and temperature in the wake of a cylinder are available. The more successful of these correlations are due to Prandtl (18), Taylor (19), Hu (17), and Townsend (9) and the results obtained by these investigations will be briefly reviewed here and compared with the correlation of Equations 37 and 50 and with the experimental data reported in this thesis.

The first reasonably successful attempt at a description of turbulent momentum transfer in the wake of a cylinder was due to Prandtl. According to the theory proposed, the distribution of velocity downstream from a cylinder is controlled by momentum transfer and is determined by the following relationship.

$$u_{oc} \frac{\partial u_d}{\partial x} = \frac{\partial}{\partial y} \left(\epsilon_m \frac{\partial u_d}{\partial y} \right) \tag{60}$$

In a further attempt to describe the turbulence processes, Prandtl introduced the concept of a mixing length to characterize the motion of eddies of fluid. The mixing length is analagous to the mean free path which characterizes molecular transport processes, and is related to the eddy viscosity in the following manner

$$l^2 \left| \frac{\partial u_d}{\partial y} \right| = \epsilon_m \tag{61}$$

Equations 60 and 61 may be combined to give a differential equation for the velocity in terms of the mixing length. Prandtl assumed that similarity obtained throughout the wake and thus that ℓ was proportional to the breadth of the wake. By dimensional analysis the width of the wake was shown to vary as $X^{\frac{1}{2}}$ and the centerline velocity deficiency, $u_c - u_{oc}$, as $x^{-\frac{1}{2}}$. With this information the solution to Equation 60 is found to have the form

$$\frac{u - u_o}{u_c - u_{oc}} = \left[1 - \left(0.441 \frac{y}{y_u} \right)^{3/2} \right]^2 \qquad (62)$$

The differences between Equation 62 and Equation 37 are solely the result of the assumptions made regarding the nature of ϵ_m. The graph of Equation 62 is shown in Figure 31, where it is seen to compare favorably with the curve of Equation 37. Reference to Figure 18 indicates that the distribution due to Prandtl does not describe the experimental velocity distributions with as great an accuracy as does Equation 37, although the scatter of the experimental points is too great to make possible the formation of any definite conclusion.

In 1932 Taylor proposed a different mechanism for turbulent transfer, according to which vorticity, rather than momentum, was conserved in the wake. The following partial differential equation embraces the principles of his vorticity transfer theory for the flow system considered here.

$$u_{oc} \frac{\partial u_d}{\partial x} = \epsilon_m \frac{\partial^2 u_d}{\partial y^2} \qquad (63)$$

It should be noted that both Equations 60 and 63 are essentially identical with Equation 33 if it is assumed that the eddy viscosity remains constant throughout the wake. However, a distribution entirely different from that of Equation 37 results if Equation 63 is solved subject to the same conditions proposed by Prandtl regarding geometrical similarity. It may be shown that the solution obtained upon substitution for ϵ_m in terms of the mixing length is indeed identical with Equation 62. Thus the two basically different schemes of turbulent transfer yield identical distributions for the velocity as a function of position downstream from a cylinder. Nevertheless, it will be shown later that the two theories lead to different distributions of temperature in the wake of a heated cylinder.

The more recent statistical descriptions of the turbulence processes (20,21,22) may also be applied to the prediction of velocity and temperature distributions in the cylinder wake. In addition to the hydrodynamic equations (e.g., Equations 19, 20, 21, and 22), expressions involving the various correlation components describing the field must be simultaneously satisfied.

Hu has applied the theory developed by Chou (22) to the analysis of the cylinder wake. Chou's theory was modified by Hu. That is, the equations involving the triple correlation coefficients were by the aid of symmetry arguments, ignored. Taylor's microscale of turbulence was assumed by Hu to be constant throughout the wake, and it was assumed that geometrical similarity existed. With these assumptions, Hu was able to arrive at a universal velocity

distribution, which for comparison with the results of this thesis, may be expressed as

$$\frac{u - u_o}{u_c - u_{oc}} = \left[\frac{2.25\left(1 - 0.1142\, Y^2/y_u^2\right)}{2.25 + 0.1142\, Y^2/y_u^2} \right]^{4.06} \qquad (64)$$

Hu determined the constants appearing in the expression by fitting a curve to the experimental data of Fage and Falkner (7). A plot of the above equation is shown in Figure 31. Upon comparison with the data of Figure 18 it appears that Equation 64 gives perhaps as good a representation of the data as does Equation 37.

Townsend (9,10) has recently performed measurements of velocity and temperature in the wake of a cylinder. Data were also obtained showing the variation of intensities and correlation coefficients across the wake. The results were analyzed and shown to indicate the coexistence of two different mechanisms of transfer. Both small and large scale fluctuations were proposed, the former being largely responsible for the ordinary production of turbulent shear. The latter motion was described by Townsend (23) as the intermittent production of large jets of fluid, originating within the highly turbulent core of the wake, and transporting the energy of the core turbulence to the outer regions of the wake. This latter mechanism was charged with the responsibility for the increased normal transfer of heat in the wake of a cylinder. The resultant of the two types of turbulent shear was characterized by the existence of a

constant, effective eddy viscosity and an intermittency factor which varied across the wake and could be represented approximately by the expression

$$\gamma = \left[1 + 3a \left(\frac{Y}{Y_n} \right)^4 \right]^{-1} \tag{65}$$

The equation describing the distribution of velocity was taken to be

$$u_{oc} \frac{\partial u_d}{\partial x} = \frac{\partial}{\partial Y} \left(\gamma \epsilon_m \frac{\partial u_d}{\partial Y} \right) \tag{66}$$

Townsend (9) was able to solve the velocity equation in the region of the wake in which geometrical similarity prevails, and the following expression follows directly from his result.

$$\frac{u - u_o}{u_c - u_{oc}} = e^{-\left(\frac{Y}{Y_n}\right)^2 \left[1 + a\left(\frac{Y}{Y_n}\right)^4 \right] \frac{\ln 2}{1+a}} \tag{67}$$

The above expression is compared in Figure 32 with the distribution of velocity predicted by Equation 37. The value of 0.0470 for the constant a was calculated from Townsend's results. Inspection indicates that the experimental velocity data are also represented reasonably well by Equation 67, although again the scatter of the data makes impossible an adequate test of this theory. The most

significant conclusion to be drawn at this point is that the shape of the mean velocity profile is relatively insensitive to the basic assumptions employed in the description of the turbulence processes.

Experiment has shown that the region of true geometrical similarity with respect to the statistical quantities of turbulence does not appear short of 500 diameters downstream (9). Evidently sufficient uniformity exists, however, so that the assumption of similarity serves to describe adequately the velocity distribution. The entire range covered in the present experimental work extends only from 15 to 170 diameters downstream from the axis of the cylinder.

The preceding theories of turbulent transfer have been extended also to the prediction of the temperature distribution downstream from a heated cylinder. The approximate equation satisfied by the temperature distribution is

$$u_{oc} \frac{\partial T}{\partial X} = \frac{\partial}{\partial Y}(\epsilon_c + k) \frac{\partial T}{\partial Y} \qquad (5)$$

The momentum transfer theory proposed by Prandtl may be shown to yield for the temperature distribution the following dimensionless relationship.

$$\frac{T - T_o}{T_c - T_o} = \left[1 - \left(0.441 \frac{Y}{Y_T} \right)^{3/2} \right]^2 \qquad (68)$$

This expression is seen to be identical in form with Prandtl's theoretical velocity distribution (Equation 62), differing only in the introduction of the characteristic temperature wake width, y_T. The primary assumption involved in the derivation of Equation 68 from the partial differential equation describing the temperature field is that the eddy conductivity and the eddy viscosity are identical throughout the wake and that the molecular viscosity and conductivity are negligible. With this assumption the temperature field may be immediately determined from a knowledge of the distribution of velocity in the wake. Equation 68 is shown for comparison with other theories in Figure 33.

The vorticity transport equations of Taylor may be manipulated under the same assumptions to yield for the temperature distribution the result

$$\frac{T - T_o}{T_c - T_o} = 1 - \left(0.630 \frac{Y}{y_T}\right)^{3/2} \qquad (69)$$

Equation 69 is plotted as a function of Y/y_T in Figure 33, and reference to Figure 20, which contains experimental temperature data, indicates that Taylor's theoretical distribution results in a very poor correlation for $Y/y_T > 1$. It is felt that the success of Taylor's theory in correlating the data of Fage and Falkner (7) is only fortuitous. Comparison of the temperature data was made on the basis of the width associated with the velocity wake. The data of this thesis indicate that such a comparison is quite invalid because

of the marked difference in the characteristic widths of the velocity and temperature wakes for any given distance downstream from the cylinder. Fage and Falkner's measurements are represented well by Prandtl's theoretical curve when plotted on the basis of the appropriate characteristic width of the wake.

Hu shows that the equation satisfied by the temperature distribution has the same form, on the basis of the statistical theory due to Chou, as the equation satisfied by the velocity. Thus the temperature is treated as a fourth component of the velocity vector, and the following dimensionless distribution is obtained.

$$\frac{T - T_0}{T_c - T_0} = \left[\frac{2.25\left(1 - 0.232\, y^2/y_T^2\right)}{2.25 + 0.232\, y^2/y_T^2} \right]^{1.91} \qquad (70)$$

The constants chosen by Hu were calculated on the basis of a comparison with Fage and Falkner's measurements. The above expression is shown in Figure 33 where it is compared with the previous distributions. There is a certain amount of speculation as to the validity of the assumptions employed by Hu to represent the temperature distribution (9). No real results of significance to the statistical theory of turbulence come from Hu's work, and it is argued that even incorrect pictures of the structure of turbulence in the wake will give correct descriptions of the distribution of macroscopic properties such as temperature and velocity.

Comparison of the temperature and velocity distributions of

Figures 31, 32, and 33 which have been derived under a host of different assumptions indicates that the prediction of point values of velocity and temperature is not extremely sensitive to the assumptions involved in the analysis of the turbulent flow field. However, the actual point values of heat and momentum transfer are somewhat more sensitive to the basic assumptions employed, and serve as a more rigorous check upon the validity of the various theories of the transfer process.

The equation for the transfer of heat by molecular and turbulent conduction normal to the plane of the cylinder wake is

$$\frac{\dot{q}_n}{c_p \sigma} = -(\epsilon_c + k) \frac{\partial T}{\partial Y} = \overline{v'T'} - k \frac{\partial T}{\partial Y} \qquad (7)$$

This expression is seen to depend explicitly upon both the point temperature in the flow field and upon the eddy conductivity. The value of $\dot{q}_n$ as a function of position in the wake may be determined directly from the differential equation for the temperature distribution. Upon integration of Equation 5 from $Y = 0$ to $Y = Y$ there results

$$-\frac{\dot{q}_n}{c_p \sigma} = (\epsilon_c + k) \frac{\partial T}{\partial Y} = \int_0^Y u_{oc} \left(\frac{\partial T}{\partial x} \right) d\xi \qquad (71)$$

If it is recognized that Equations 50, 68, 69, and 70 all contain

implicitly the following two conditions

$$T_c - T_o = \text{const}_1 \; x^{-\frac{1}{2}} \tag{72}$$

$$Y_T = \text{const}_2 \; x^{\frac{1}{2}} \tag{73}$$

then they may all be manipulated in a similar fashion to yield simple expressions for the normal heat flux in the wake. The results obtained by application of Equation 71 to each of the theoretical distributions are

$$(\epsilon_c + k)\frac{\partial T}{\partial y} = \frac{u_{oc}(T_c - T_o) Y_T}{2x} \frac{y}{Y_T} e^{-\left(\frac{y}{Y_T}\right)^2 \ln 2} \quad \text{(This thesis)} \tag{74}$$

$$(\epsilon_c + k)\frac{\partial T}{\partial y} = \frac{u_{oc}(T_c - T_o) Y_T}{2x} \frac{y}{Y_T}\left[1 - \left(0.441 \frac{y}{Y_T}\right)^{3/2}\right]^2 \quad \text{(Prandtl)} \tag{75}$$

$$(\epsilon_c + k)\frac{\partial T}{\partial y} = \frac{u_{oc}(T_c - T_o) Y_T}{2x} \frac{y}{Y_T}\left[1 - \left(0.630 \frac{y}{Y_T}\right)^{3/2}\right] \quad \text{(Taylor)} \tag{76}$$

$$(\epsilon_c + k)\frac{\partial T}{\partial y} = \frac{u_{oc}(T_c - T_o) Y_T}{2x} \frac{y}{Y_T}\left[\frac{2.25\left(1 - 0.232\, y^2/Y_T^2\right)}{2.25 + 0.232\, y^2/Y_T^2}\right]^{1.91} \quad \text{(Hu)} \tag{77}$$

It is noteworthy that the quantity $(\epsilon_c+\kappa)\frac{\partial T}{\partial Y}\frac{2x}{u_{oc}(T_c-T_o)Y_T}$ is for each theory a function only of the fractional position in the wake, Y/Y_T, indicating that similarity does exist with respect to the dimensionless heat flux. Equations 74, 75, 76, and 77 form the basis of Figure 34 in which the theoretical equation developed in this thesis is indicated by the solid line. There appears to exist a greater divergence of the theories in the region $\frac{Y}{Y_T} > 1,5$ than is found to exist for the correlation of point temperatures in the wake.

Although Townsend (9) gives no expression for the temperature distribution or for the turbulent heat flux, he has measured the heat flux in the wake of a 0.0625 inch diameter cylinder, and his results are in reasonable quantitative agreement with the curves of Hu and Prandtl shown in Figure 34.

The experimental data presented in this thesis are sufficient for the calculation of point values of heat flux in the cylinder wake. With the neglect of conduction in the downstream direction Equation 45 becomes

$$\frac{\partial}{\partial Y}(\epsilon_c+\kappa)\frac{\partial T}{\partial Y} = u\frac{\partial T}{\partial X} + v\frac{\partial T}{\partial Y} \qquad (78)$$

The normal convective term, $v\frac{\partial T}{\partial Y}$, may not be neglected. Although this term does not contribute noticeably to the calculation of temperature distribution, it has an appreciable effect upon the calculation of normal heat flux. The continuity equation in two

dimensions may be written for symmetric steady flow as

$$v = -\int_0^Y \left(\frac{\partial u}{\partial x}\right) d\xi \tag{79}$$

If Equations 78 and 79 are combined and integrated from $Y = o$ to $Y = Y$ the following result is obtained

$$(\epsilon + k)\frac{\partial T}{\partial Y} = \int_0^Y u\left(\frac{\partial T}{\partial x}\right) d\eta - \int_0^Y \left(\frac{\partial T}{\partial Y}\right)\left[\int_0^\eta \left(\frac{\partial u}{\partial x}\right) d\xi\right] d\eta \tag{80}$$

This expression, together with derivatives of temperature and velocity obtained from the experimental data, has been used to establish the normal heat flux in the wake. Figure 35 presents the results of the calculations for six traverses at the nominal air speed of 30 feet per second. The results have been expressed in dimensionless form for comparison with the theoretical expression of Equation 74. The lowest set of points shown represents values of the heat flux for the traverse 1/2 inch downstream from the midline of the cylinder, and indicate that similarity has not yet been attained at this point. Nevertheless, the remaining points (for traverses further downstream) indicate that similarity does indeed exist. Agreement with the theoretical relationship is good, and it is evident that the expressions developed are sufficiently accurate for an adequate description of both point temperatures and point values of the heat flux.

In the region of the wake in which $\frac{Y}{Y_T} < 1$ it is seen from Figures 34 and 35 that the theoretical relations of Taylor, Prandtl, and Hu also describe the heat flux with accuracy. However, agreement fails in the region $\frac{Y}{Y_T} > 1.5$. It is hoped that further experimental investigation of the point behavior of turbulent heat transport will be undertaken, since such knowledge is fundamental to the understanding of the mechanisms of transfer in the wake of a cylinder. In particular, the experimental techniques developed by Townsend (9,10,23) provide a means for the direct measurement of the contribution of turbulence to the normal heat transport. It is noteworthy that the experiments of Townsend (9) indicate that the distribution of heat flux is not similar for at least 500 diameters downstream.

The normal heat flux has also been calculated on the basis of values of eddy conductivity determined for free channel flow in the same apparatus (33). The shape of the eddy conductivity distribution was similar to that of Figure 42. The derivatives of the temperature were obtained from the temperature data reported here. In this case the heat flux was taken to be

$$\frac{\dot{q}_n}{c_p \sigma} = -(\epsilon_t + k)_u \frac{\partial T}{\partial y} \qquad (81)$$

Figure 36 contains values of $\dot{q}_n$ for five traverses at a nominal velocity of 30 feet per second. The dimensionless form of presentation has been utilized, and agreement with the theoretical curve (Equation 74) is reasonably good. However, the disagreement in

the region $y/y_\tau < 0.6$ indicates that the uniform flow eddy conductivity distribution is too small, whereas near $y/y_\tau = 1$ the eddy quantity appears to be somewhat too large. This would appear to indicate quantitatively that there is produced a region of relatively higher turbulence immediately downstream from the cylinder.

It is to be noted here that the zero value of the heat flux at the center of the wake does not imply that the eddy conductivity becomes zero at this point, but is a result of the vanishing of the temperature derivative. Indeed, were the eddy conductivity to reach zero, the heat flux would not only vanish, but show also a nearly zero derivative at the center. This result may be seen by consideration of the following expression for the derivative of $\dot{q}_n$.

$$\frac{1}{c_p \sigma} \frac{\partial \dot{q}_n}{\partial Y} = -(\epsilon_c + K) \frac{\partial^2 T}{\partial Y^2} - \frac{\partial \epsilon_c}{\partial Y} \frac{\partial T}{\partial Y} \qquad (82)$$

By symmetry it is evident that both $\frac{\partial T}{\partial Y}$ and $\frac{\partial \epsilon_c}{\partial Y}$ are zero when $Y = 0$. Thus, for $Y = 0$, the derivative of $\frac{1}{c_p \sigma} \dot{q}_n$ with respect to Y would reduce to $K \frac{\partial^2 T}{\partial Y^2}$. This quantity, at a nominal velocity of 30 feet per second, is only about 4% of the observed value of $\frac{1}{c_p \sigma} \frac{\partial \dot{q}_n}{\partial Y}$, indicating that ϵ_c indeed does not vanish at the center of the wake.

Prediction of Temperature Gradients in Uniform Flow

The ability to predict with accuracy point values of temperature and of thermal flux is often of paramount importance in designs involving turbulent transfer. The majority of such problems confronting the chemical engineer are concerned with non-uniform phenomena, and often are of such complexity as to preclude any exact analytical treatment. Nevertheless these problems must be solved at least approximately before the engineer is able to reach any reasonable understanding of the importance of end effects and other disturbances in the design of heat exchanging equipment.

The purpose of this section is to review the application of electric analog methods (28) to the prediction of heat transfer under cases of non-uniform temperature distribution, and to present the results of one such study carried out at the California Institute of Technology. It is hoped that the ideas contained herein will serve to stimulate interest in this field of analysis and to provide sufficient background information to encourage further applications of such methods in the field of non-uniform transfer of heat to turbulently flowing fluids. It should be pointed out that the methods reviewed here may be applied with equal success to the determination of concentrations and to the evaluation of material transfer under a number of similar cases of engineering interest. For simplicity the ensuing material will be restricted to a consideration of the problems of heat transfer, although the extension to diffusion problems should be obvious.

The following discussion concerns the use of an electric analog computer (29) for the solution of the following equation

$$\frac{\partial}{\partial Y}(\epsilon_c + K)\frac{\partial T}{\partial Y} = u\frac{\partial T}{\partial X} \qquad (83)$$

which describes the temperature field in the case of a fluid flowing uniformly between parallel plates when conduction in the direction of main flow can be neglected. It has also been assumed that the properties of the fluid remain constant throughout the region considered.

The principles underlying the successful application of electric analog methods to the solutions of ordinary and partial differential equations and the corresponding boundary value problems which describe physical processes are not new. It has long been realized that the equations which govern the distribution of voltage and current in electrical networks are similar if not identical in form to many other equations of mathematical physics. Hence, the solution to a given problem may often be identified with the solution to a corresponding problem of electricity. The analogy does not stop here. In fact, a host of analog methods are at present employed in the solution of problems of physical interest, the merit of the individual method being measured in a large part by the ease with which a solution may be obtained (26,27).

The electric analog computer, being well adapted to the study of transient phenomena is particularly convenient for the solution

to the problems of non-uniform heat transfer. The wide variety of electrical components available to the ingenious operator makes it possible to treat satisfactorily problems which involve rather complex initial temperature distributions and boundary conditions. Depending upon the total number of elements employed in the computer circuit it is possible to represent to varying degrees any initial temperature distribution involved in the solution to Equation 83. Likewise, by the application of arbitrary function generators, virtually any temperature boundary conditions may be applied to a given problem. It is not difficult to realize the possibility of applying conditions of variable heat flux across the boundaries of the system. Such boundary conditions are encountered in physical situations in which the surface temperature of the system is unknown, but from which there is a transfer of heat to constant temperature surroundings. The surface heat transfer coefficient may be a constant or a function of time.

Solutions obtained by the use of the analog computer are not exact for several reasons. They do not take into account any nonlinearities entering through variation of the properties of the fluid with temperature, nor do they consider conduction downstream or variations of ϵ_c and u in the direction of flow, although it is possible to include the latter through use of sufficiently complex networks. For the computer considered here it is necessary to represent the partial differential equation by its finite difference counterpart. The convergence of such methods to the solutions of

the original equations has been discussed (43,44). Such limitations are inherent in the method, and cannot be resolved. In addition, practical considerations generally prohibit the use of precision components in the computer, with the result that the accuracy of the solution is decreased. In situations where solutions of greater accuracy are desired, one must in general turn to numerical methods, including use of sequence controlled, high speed digital computers (25). However, it is important to note than an approximate solution in such a case from the analog computer, when used as a starting point for the more exact methods, will hasten the convergence for the solution to such an extent that very little additional effort will be required.

For the solution to Equation 83 it is convenient to use a network of elements as shown in Figure 37C. Application of Kirchhoff's law to the nth node yields the following relation between the voltages and the time

$$\frac{E_{n+1} - E_n}{\Delta R_{n,n+1}} - \frac{E_n - E_{n-1}}{\Delta R_{n-1,n}} = C_n \frac{\partial E_n}{\partial \theta} \qquad (84)$$

If $\Delta R_{n,n+1}$ is now chosen to be equal to $\Delta R_{n-1,n}$ the equation may be written as

$$\frac{E_{n+1} - 2E_n + E_{n-1}}{\Delta R} = C_n \frac{\partial E_n}{\partial \theta} \qquad (85)$$

which is readily recognized to be a finite difference counterpart of the equation

$$\Delta R \frac{\partial^2 E}{\partial R^2} = C \frac{\partial E}{\partial \theta} \tag{86}$$

Hence, if Equation 83 can be reduced to this form, by application of proper boundary conditions to the circuit (Figure 37C) a reasonably accurate solution to the heat transfer problem may be obtained. This result may be achieved by defining a new independent variable $\varphi\left(\frac{Y'}{Y_0}\right)$ by the relation

$$\varphi\left(\frac{Y'}{Y_0}\right) = \int_0^{Y'/Y_0} \frac{1}{\epsilon_c(\xi)+K}\, d\xi \tag{87}$$

Equation 83 now assumes the form

$$\frac{\partial^2 T}{\partial \varphi^2} = Y_0^2\, u(\varphi)\left[\epsilon_c(\varphi)+K\right]\frac{\partial T}{\partial X} \tag{88}$$

and the similarity with Equation 86 is evident. The correspondence is complete on identification of φ with R, $u(\epsilon_c+K)$ with C, and X with time. That such identification is reasonable is apparent. Equal increments of φ represent equal units of resistance to heat flow across the channel; accumulation of charge on the capacitors is identified with the sweeping of heat downstream by the motion of the fluid. The voltage distribution as a function of time in the system is similar to the state of affairs observed by an individual moving downstream with the fluid.

To complete the solution it is necessary to have available values for the eddy conductivity and the velocity as functions of position in the channel, and to achieve the proper correspondence with respect to the physical boundary conditions.

Since it is desired to illustrate the use of the analog computer by solution of a heat transfer problem for which experimental temperature distributions are actually available, a review of the experimental work will be given here.

Measurements have been made (30) of the distributions of temperature and velocity as functions of position in a turbulently flowing air stream. The experimental apparatus utilized was the same as that described in an earlier section of this thesis. For the experiments, three different boundary conditions were investigated. These were 100/85/100, 100/100/85, and 115/100/85, in which the three numbers indicate nominally the temperatures of the upper plate, the entering air, and the lower plate, respectively. Figure 37A indicates schematically the conditions existing at the entrance to the "heated section." Traverses of temperature and velocity were made at several different stations downstream from the entrance to the heated section to determine the nature of the temperature distribution during the region of non-uniform transfer of heat. Three of the experimental velocity traverses are indicated in Figure 38 and show that the velocity profile was substantially developed at the region of interest. The experimental temperature traverses are shown in Figures 39, 40, and 41. The experimental

data for successive stations downstream from the entrance to the heated section have been separated from one another by a constant amount in Figures 40 and 41 to facilitate comparison with the results of the analog calculation.

To solve Equation 83 it is necessary to have available values for ϵ_c and u as functions of Y'. To achieve best correspondence with the experimental data, the velocity distribution was chosen as in Figure 38 (heavy line) which represents an arithmetic average of the distributions obtained in the experimental work. Values for the eddy conductivity were taken from a correlation of ϵ_c as a function of Y' and of the Reynolds number based upon the bulk velocity. These values had their origin in measurements (33) involving uniform transfer of heat. Figure 42 gives the distribution used in the calculations.

From a knowledge of ϵ_c as a function of Y' the variable φ may be determined, and once a choice of the total number of circuit elements is made, the appropriate value of $\Delta\varphi$ may be obtained. The capacitance at the nth node is determined from the relation

$$C_n = \frac{(\Delta\varphi)^2}{\Delta R} \frac{Y_o^2}{\lambda} (\epsilon_c + \kappa)_n u_n \qquad (89)$$

In the above expression ΔR is the resistance between two nodes and λ is the conversion factor relating time in the electrical circuit to distance in the boundary value problem.

The only limitations upon the choice of the numerical values

of ΔR and C_n are practical ones; i.e., the choice is usually dictated by the range of R and C components available, the time sensitivity of the switches used, and the desired sweep time of the oscilloscope used to trace node voltages as a function of time. If R is large and C is small, leakage of charge from the circuit may appreciably affect the accuracy of the solution.

For the work reported here the values chosen were

$$\Delta R = 46 \text{ ohms} \qquad \lambda = 1000 \text{ in/sec} \qquad n = 25$$

The corresponding values of C_n were calculated on this basis, and are listed in Table III.

To represent properly the physical boundary conditions prevailing it was necessary to consider the existence of resistance to heat transfer in the oil baths, since it was known experimentally (30) that the plate temperatures were not uniform with respect to downstream distance under non-uniform heat transfer conditions particularly near the entrance to the heated section.

Ideally, the distribution in the oil baths should be represented by use of additional circuit elements. However, as the oil flows countercurrent to the air stream such a procedure would require the use of negative capacities, the use of which, though not impossible, was not practicable in the present study. Thus, rather than represent point temperatures in the oil streams, the problem was solved by choice of appropriate boundary conditions at the oil bath - copper plate face. It was assumed that the bulk temperatures of the oil

baths were substantially constant over the range studied and resistance to heat flow was assumed to reside wholly in an oil film next to the plate. The heat transfer coefficient for this film was determined from previous uniform transfer studies in this laboratory.

Consider the boundary of the system at any point downstream from the channel entrance. Because the conditions are constant with respect to time, the total heat flux to the air stream at a wall must be identical with the heat flux to the wall from the oil bath. The boundary condition at one wall is (Figure 43)

$$\dot{q} = -C_p \sigma K \left.\frac{\partial T}{\partial Y}\right|_{WALL} = h_{OIL}(T_W - T_{OIL}) \qquad (90)$$

In the steady state case, this condition must be true at all downstream positions. Referring to Figure 37C, the above condition may be interpreted also in terms of voltages as

$$\frac{E_B - E_1}{R_W} = \frac{E_1 - E_2}{\Delta R} \qquad (91)$$

The latter condition is automatically satisfied if there is no charge drain at node 1. Node 1 then corresponds to the channel wall, and point B to the oil bath.

If Equation 90 is written in difference form it becomes

$$h_{OIL}(T_{OIL} - T_W) = \frac{C_p \sigma K}{\Delta Y_{WALL}}(T_W - T_2) \qquad (90a)$$

Hence

$$\frac{T_{oil} - T_w}{T_w - T_2} = \frac{c_p \sigma}{h_{oil} Y_o \Delta \varphi} \tag{92}$$

There exists a linear correspondence between E and T so that

$$T = AE + B \tag{93}$$

Upon substitution of this relationship into Equation 92 there is obtained

$$\frac{T_{oil} - T_w}{T_w - T_2} = \frac{E_B - E_1}{E_1 - E_2} = \frac{c_p \sigma}{h_{oil} Y_o \Delta \varphi} = \frac{R_w}{\Delta R} \tag{94}$$

The equation determining R_w is thus

$$R_w = \frac{c_p \sigma}{h_{oil} Y_o \Delta \varphi} \Delta R \tag{95}$$

The above relationship was used to establish the proper values of R_w for each boundary condition. The boundary conditions studied included three different bath temperatures. The corresponding heat transfer coefficients varied, and R_w was changed for each condition. Because of some uncertainty in the values used for h_{oil}, and in the thickness of the laminar layer in the air stream each set of temperature conditions was run a second time with wall resistance three times the value originally chosen. Table IV contains a tabulation of the values of R_w used in the solution for each condition.

The temperature boundary conditions studied corresponded to the experimental conditions 115/100/85, 100/100/85, and 100/85/100. Since the analog solution is based on a linear relationship between temperature and voltage, the actual conditions on the analog were chosen as $+E_B$/ground /$-E_B$,ground /ground/$+E_B$, and $+E_B$/ ground /$+E_B$. In the three cases, ground corresponded to 100°F, 100°F, and 85°F, respectively.

The circuit elements were connected as shown in Figure 37C and for each boundary condition the proper value of R_W was chosen. One beam of a double beam oscilloscope was connected to the node whose potential was desired and the battery switches were closed. A photograph was taken of the beam trace on the oscilloscope. Figure 44 is a sample photograph. Data were obtained at alternate nodes in the circuit.

For each case photographs were made of the voltage at B (Figure 37C) which corresponded to the forcing function, and hence served as a calibration scale on the subsequent photographs. Because of the variation in voltage across the network it was advisable to use different gain and signal attenuations at different nodes to facilitate reduction of the data. Calibration of these controls was made separately.

By adding an inductance-capacitance series leg to the circuit (Figure 37C) and connecting this leg to the second beam of the scope it was possible to place a timing signal alongside the voltage trace on each photograph. The theory of such a circuit is well known (45)

and the frequency of the sine wave produced may be readily calculated from the circuit constants. The wave shown in Figure 44 has a frequency of 402.6 cycles per second, each cycle corresponding to approximately 30 inches distance down the channel.

Data were taken directly from the photographic negatives using a large magnifying glass and a pair of dividers. Voltages were read at points corresponding to the stations at which experimental data were available. Conversions to temperature were made with the calibration constants for each set of boundary conditions.

A comparison of wall temperatures calculated by the analog method with experimental values indicated that the true resistance in the neighborhood of the wall was approximately the arithmetic mean of the values chosen for the analog solution. Consequently, comparison with experiment has been made on this basis. The difference has been attributed to uncertainties in the thickness of the laminar film in the air stream, and amounts to a 10% change in this region of high resistance. Reported temperatures are the average of the values found for the two cases at each of the boundary conditions studied. Figure 37B contains a plot of the experimental and the calculated values of wall temperature as a function of downstream distance for the condition 100/85/100. It is felt that the agreement is quite satisfactory.

Figures 39, 40, and 41 are a comparison of the analog calculation with the experimental data of Mason (30) taken under the same conditions. Agreement with experiment is excellent, especially in

the case 100/85/100 which represents the most stringent test of the solution. In particular, the calculated curves show the same characteristic variations in curvature which are exhibited by the experimental data. This somewhat peculiar phenomenon results from the actual shape of the eddy conductivity distribution. Because of uncertainties associated with the absolute values of the experimental temperatures used for comparison, the 100/100/85 and the 115/100/85 cases have been compared on a relative basis only. For the former case the experimental and calculated solutions were made to agree at the point $\frac{y'}{y_o} = 0.950$, while in the latter case, agreement was set at the centerline of the channel. The nature of the experimental uncertainties was such that for both cases the method of adjustment of the analog solution consisted of the addition of a constant term to each calculated temperature.

It is possible to determine the heat transfer coefficient for the 100/85/100 case directly from the analog solution eliminating the necessity for calculations of bulk temperatures. The heat transfer coefficient, h, is defined by means of the following series of relationships

$$h(T_w - T_{mc}) = \dot{q} = -c_p \sigma k \frac{\partial T}{\partial Y}_{WALL} = h_{OIL}(T_{OIL} - T_w) \quad (96)$$

where T_{mc} is the mixing-cup temperature which may be expressed as follows

$$T_{mc} - T_o = \frac{1}{u_B} \int_0^1 u(T - T_o) \frac{dY'}{Y_o} \quad (97)$$

with

$$u_B = \int_0^{1} u \, \frac{dY'}{Y_0} \tag{98}$$

T_{mc} is that uniform temperature which the fluid would assume upon discharge from the section in question into an insulated receiver.

Since there exists a linear relationship between E and T as given by Equation 93 we may write

$$T_{mc} - T_0 = AE_{mc} \tag{99}$$

where A is determined from the calibration data. The right side of Equation 99 does not contain the term E_0 since for the case considered E_0 was taken to be zero (ground). Now E_{mc} is also that voltage which would obtain in the analog circuit if the circuit were located at a particular instant, θ, and may therefore be established from the following relation

$$E_{mc} = \frac{\text{total charge}}{\text{total capacitance}} = \frac{2}{C} \int_0^{\theta} i' \, d\xi \tag{100}$$

where

$$C = \sum_n C_n \tag{101}$$

Recognizing that the current flowing into the circuit from one end is expressed by

$$i' = \frac{E_B - E_1}{R_W} = \frac{\Delta E_W}{R_W} \tag{102}$$

and that

$$\lambda = \frac{dX}{d\theta} \tag{103}$$

Equations 97, 99, 100, 102, and 103 may be combined to yield

$$T_{mc} = T_o + \frac{2A}{\lambda R_w \subseteq} \int_0^X \Delta E_w \, d\xi \tag{104}$$

Upon substitution of the above relationship into Equation 96 there is obtained, with some rearrangement, the following relationship.

$$\frac{h}{h_{oil}} = \frac{T_{oil} - T_w}{(T_{oil} - T_o) - (T_o - T_w) - \frac{2A}{\lambda R_w \subseteq} \int_0^X \Delta E_w \, d\xi} \tag{105}$$

Since for the temperature boundary condition 100/85/100 the value of $T_{oil} - T_o$ is 15°F, Equation 105 may be further simplified to yield the final expression

$$\frac{h}{h_{oil}} = \frac{\Delta E_w}{\frac{15}{A} - \Delta E_w - \frac{2}{\lambda R_w \subseteq} \int_0^X \Delta E_w \, d\xi} \tag{106}$$

for the heat transfer coefficient for the air stream as a function of the oil bath coefficient, h_{oil}, and the direct information obtained from the analog solution. Figure 45 shows a plot of the heat transfer coefficient h for the air stream as a function of distance downstream from the entrance to the heated section. The prediction of McAdams (1) is indicated. The inadequacy of the correlation of McAdams in the region less than forty diameters downstream is apparent.

Conclusions

The results of this thesis indicate the possibility of predicting with reasonable accuracy distributions of temperature, velocity, and concentration in turbulent fluid systems. The descriptions are found to be good even in those cases in which it is known that the assumptions necessary for simple analytical treatment are poor. It is emphasized that analytical distributions of mean velocity and temperature in the wake of a heated body are relatively insensitive to the assumptions made regarding the actual nature of the turbulence processes, and profiles derived under a number of different assumptions are shown to have nearly identical forms.

It is suggested that further investigations be undertaken to determine both the effects of intensity and scale of turbulence upon the overall heat transfer characteristics of cylinders and other shapes. Although some such work of this type has been reported (35), it is not considered to be complete. The disagreement between the values for the heat transfer coefficient reported in this thesis and the values predicted by McAdams indicate that the structure of the turbulent field is important in determining the heat transfer characteristics of cylinders.

A more complete investigation of the heat transfer as a function of position in the wake of a cylinder should be conducted. In particular, direct measurements of the turbulent heat flux may be obtained (9), and these may be used to test further the usefulness

of the theories of transfer in the cylinder wake. Although the values of heat flux in the wake calculated from the data included here agree with the theoretical predictions developed, it is recognized that the effect of the peculiar geometry of the equipment utilized may well invalidate any conclusions which might be drawn. Measurements in an unconfined stream, especially direct measurements of the heat flux, would be desirable.

The analog computer is well adapted for the solution of the heat conduction equations for turbulent fluid systems, and is a particularly useful tool for the direct utilization of information concerning the point variations of the eddy conductivity and the eddy viscosity. The computer also provides a simple method for the analysis of the behavior of systems in which end effects or entrance effects are controlling. In systems of this type, the simplifications usually introduced for the calculation of heat transfer coefficients are not valid.

Nomenclature

English letters

a	dimensionless constant
A	calibration constant for analog computer, ^{o}F/volt
B	calibration constant for analog computer, ^{o}F
C_p	isobaric heat capacity, Btu/lb ^{o}F
C	molal concentration of natural gas, mol/ft^3
C_o	initial molal concentration of natural gas, mol/ft^3
C_m	maximum molal concentration of natural gas at any downstream distance, mol/ft^3
C_n	capacitance at n^{th} node, microfarads
d	diameter of small cylinder, in or ft
d_L	diameter of large cylinder, in or ft
d_s	diameter of sphere, in or ft
d_J	diameter of gas injection tube, in or ft
D	molecular diffusivity, ft^2/sec
E	voltage, volts
E_B	battery voltage, volts
E_n	voltage at n^{th} node, volts
g	local gravity, ft/sec^2
h	overall heat transfer coefficient, Btu/sec ^{o}F ft^2
h_c	heat transfer coefficient for cylinder, Btu/sec ^{o}F ft^2
h_{oil}	oil side heat transfer coefficient, Btu/sec ^{o}F ft^2

k_f	thermal conductivity evaluated at mean of free stream temperature and average cylinder surface temperature, Btu/sec ^{o}F ft^2/ft
l	Prandtl mixing length, in or ft
L	heated length of cylinder, in or ft
$\underline{n}$	mole fraction natural gas
$\underline{n}_o$	initial mole fraction natural gas
$\underline{n}_m$	maximum mole fraction natural gas at any downstream distance
n	a subscript indicating nth node in analog circuit
p	pressure, lb/in^2 or lb/ft^2
$\dot{q}$	rate of heat transfer per unit area, Btu/sec ft^2
$\dot{q}_n$	rate of normal heat transfer per unit area, Btu/sec ft^2
$\dot{Q}_c$	rate of heat transfer from cylinder by conduction and convection, Btu/sec
$\dot{Q}_s$	rate of heat transfer from sphere by conduction and convection, Btu/sec
r	position variable, radius, $\sqrt{x^2+y^2}$, in or ft
R	resistance, ohms
R_c	characteristic width of concentration wake, in or ft
R_w	wall resistor in analog circuit, ohms
ΔR	resistance between nodes in analog circuit, ohms
$\Delta R_{n,n+1}$	resistance between nth and n+1st node in analog circuit, ohms
s	a position variable, general, in or ft
T	time average temperature at a point, ^{o}F
T'	instantaneous temperature at a point, ^{o}F

T_c	temperature at center of wake at any distance downstream, ^oF
T_m	maximum temperature in wake at any distance downstream, ^oF
T_{mc}	mixing cup temperature, ^oF
T_n	temperature at position corresponding to n^{th} node in analog circuit, ^oF
T_o	initial or free stream air temperature, ^oF
T_{oil}	bulk temperature of oil bath, ^oF
T_s	avarage surface temperature of cylinder, ^oF
T_w	channel wall temperature (air stream side), ^oF
T'	instantaneous fluctuating component of T, ^oF
u, v, w	time average components of velocity vector at a point in X, Y, Z, directions, respectively, ft/sec
U, V, W	instantaneous components of velocity vector at a point, ft/sec
u_c	centerline velocity at any distance downstream, ft/sec
u_d	deficiency velocity, $u_o - u$, ft/sec
u_n	velocity at position corresponding to n^{th} node in analog circuit, ft/sec
u_o	free stream velocity, ft/sec
u_{oc}	maximum free stream velocity, ft/sec
u', v', w'	instantaneous fluctuating components of U, V, W, ft/sec
X, Y, Z	position variables (Figure 14), in or ft
X_o, X_o'	coordinate of virtual origin, in or ft
Y'	position variable measured from lower wall of channel, in or ft
Y_o	height of channel at any value of X, Z, in or ft

X, Y, Z	X, Y, Z components of external force, lb
Y_T, Y_u	characteristic widths of temperature and velocity wakes, in or ft

Greek letters

γ	intermittency factor
ϵ_c	eddy conductivity, ft^2/sec
$\epsilon_{cx}, \epsilon_{cy}, \epsilon_{cz}$	components of eddy conductivity in non-isotropic field, ft^2/sec
$(\epsilon_c+K)_n$	total conductivity at position corresponding to n^{th} node in analog circuit, ft^2/sec
$(\epsilon_c+K)_u$	total conductivity determined from uniform flow measurements, ft^2/sec
ϵ_D	eddy diffusivity, ft^2/sec
ϵ_m	eddy viscosity, ft^2/sec
$\epsilon_{m_{xx}}, \epsilon_{m_{xy}} \cdots$	components of eddy viscosity in non-isotropic field, ft^2/sec
η	dummy variable of integration, any units
θ	time, sec
K	thermometric conductivity, ft^2/sec
λ	factor relating distance to time in analog circuit, in/sec
μ_f	fluid viscosity evaluated at mean of free stream temperature and average cylinder surface temperature, lb/ft sec
ν	kinematic viscosity, ft^2/sec
ξ	dummy variable of integration, any units
ρ	density, lb sec^2/ft^4
σ	specific weight, lb/ft^3

τ	shearing stress, lb/ft^2
τ_n	normal shearing stress, parallel to XZ plane, lb/ft^2
$\varphi(\frac{Y'}{Y_o})$	resistance variable for analog circuit, sec/ft^2
$\Delta\varphi$	increment in φ between nodes in analog circuit, sec/ft^2

Miscellaneous

$\ln$	natural logarithm
$\overline{(\ )}$	denotes time average of quantity under bar
$\lvert(\ )\rvert$	denotes absolute value of quantity between bars

References

1. McAdams, W. H., Heat Transmission, McGraw-Hill (1942).

2. Sherwood, T. K., Absorption and Extraction, McGraw-Hill (1937).

3. Bakhmeteff, B. A., The Mechanics of Turbulent Flow, Princeton University Press, (1941).

4. von Kármán, Th., Trans. A.S.M.E., 61, 705 (1939).

5. Dryden, H. L. and A. M. Kuethe, N.A.C.A. Tech. Report No. 320 (1929).

6. Billman, G. W., D. M. Mason, and B. H. Sage, Chem. Eng. Prog., 46, 625 (1950).

7. Fage, A. and V. M. Falkner, Proc. Roy. Soc., London, A135, 702 (1932).

8. Gran Olsson, R., Zeitschr. f. angew. Math. u. Mech., 16, 257 (1936).

9. Townsend, A. A., Aust. J. Sci. Res., A2, 451. (1949).

10. Townsend, A. A., Proc. Roy. Soc., London, A190, 551 (1947).

11. Schlichting, H., Ingenieur-Archiv, 1, 533 (1930).

12. Billman, G.W., Ph. D. Thesis, California Institute of Technology (1948).

13. Mason, D. M., Ph. D. Thesis, California Institute of Technology (1949).

14. Rouse, Hunter, Elementary Mechanics of Fluids, John Wiley & Sons (1946).

15. Goldstein, S., Modern Developments in Fluid Dynamics, Oxford University Press (1938).

16. Schlichting, H., Lecture Series on Boundary Layer Theory, N.A.C.A. Tech. Memo Nos. 1217, 1218 (1949).

17. Hu, N., Chinese J. Phys., 5, 1 (July, 1944).

18. Prandtl, L., Verh. des 2. Intern. Kong. fur Tech. Mech., Zurich (1926).

19. Taylor, G. I., Proc. Roy. Soc., London, A135, 685 (1932).

20. Taylor, G. I., Proc. Roy. Soc., London, A151, 421 (1935).

21. von Kármán, Th., Journal of Marine Research, Vol. VII, No. 3, 252 (1948).

22. Chou, P.Y., Chinese J. Phys., 4, 1 (1940).

23. Townsend, A. A., Proc. Roy. Soc., London, A197, 124 (1949).

24. Jakob, M., Heat Transfer, John Wiley & Sons (1949).

25. Ridenour, L. N., J. App. Phys., 21, 263 (1950).

26. Moore, A. D., Trans. A.S.M.E., 72, 291 (1950).

27. Kayan, C. F., Trans. A.S.M.E., 71, 9 (1949).

28. McCann, G. D. and C. H. Wilts, J. App. Mech., 16, 247 (1949).

29. McCann, G. D., C. H. Wilts, and B. N. Locanthi, Proc. I.R.E., 37, 954 (1949).

30. Mason, J. L., Ph. D. Thesis, California Institute of Technology (1950).

31. Corcoran, W. H., Ph. D. Thesis, California Institute of Technology (1948).

32. King, L. V., Phil. Trans. Roy. Soc., London, A214, 373 (1914).

33. Page, Franklin, Ph. D. Thesis, California Institute of Technology (1950).

34. Berry, V. J., Student Report No. 300, Department of Chemical Engineering, California Institute of Technology (1949).

35. Comings, E. W., J. T. Clapp, and J. F. Taylor, Ind. Eng. Chem., 40, 1076 (1948).

36. Reynolds, Osborne, Phil. Trans. Roy. Soc., London, 174, 935 (1883).

37. Lamb, H., Hydrodynamics, Dover (1945) 6th revised ed.

38. Carslaw, H. S., and J. C. Jaeger, The Conduction of Heat in Solids, Oxford University Press (1947).

39. Schubauer, G. B., N.A.C.A. Tech. Report No. 524 (1935).

40. Baer, D. H., W. G. Schlinger, V. J. Berry, and B. H. Sage, "Temperature Distribution in the Wake of a Heated Sphere", To be submitted to the Journal of Applied Mechanics.

41. Schlinger, W. G. and B. H. Sage, Progress Report No. 4-108, Jet Propulsion Laboratory, California Institute of Technology (1949).

42. Unpublished data, Department of Chemical Engineering, California Institute of Technology.

43. Southwell, R. V., Relaxation Methods in Engineering Science, Oxford University Press (1940).

44. Southwell, R. V., Relaxation Methods in Theoretical Physics, Oxford University Press (1946).

45. Jeffreys, H. and B. S. Jeffreys, Methods of Mathematical Physics, Cambridge University Press (1950).

List of Figures

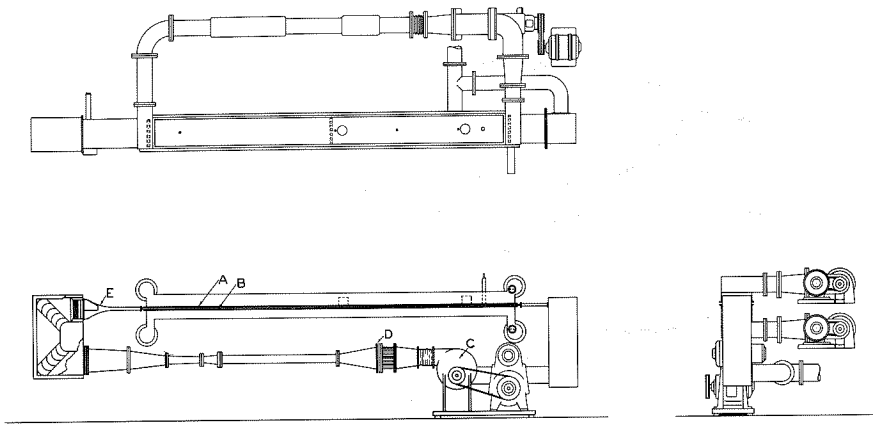

Figure 1. Essential Features of the Apparatus

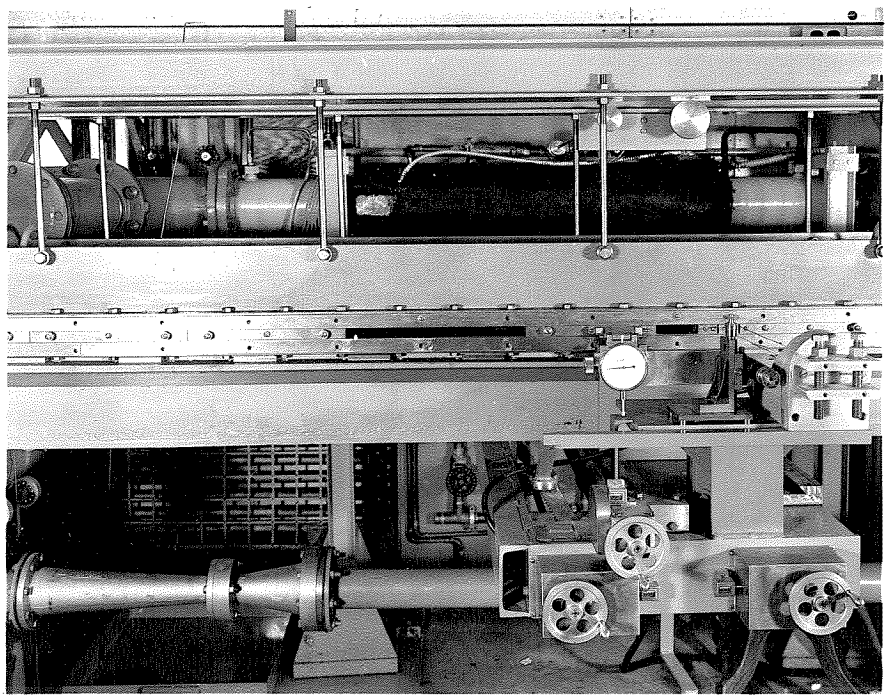

Figure 2. The Working Section

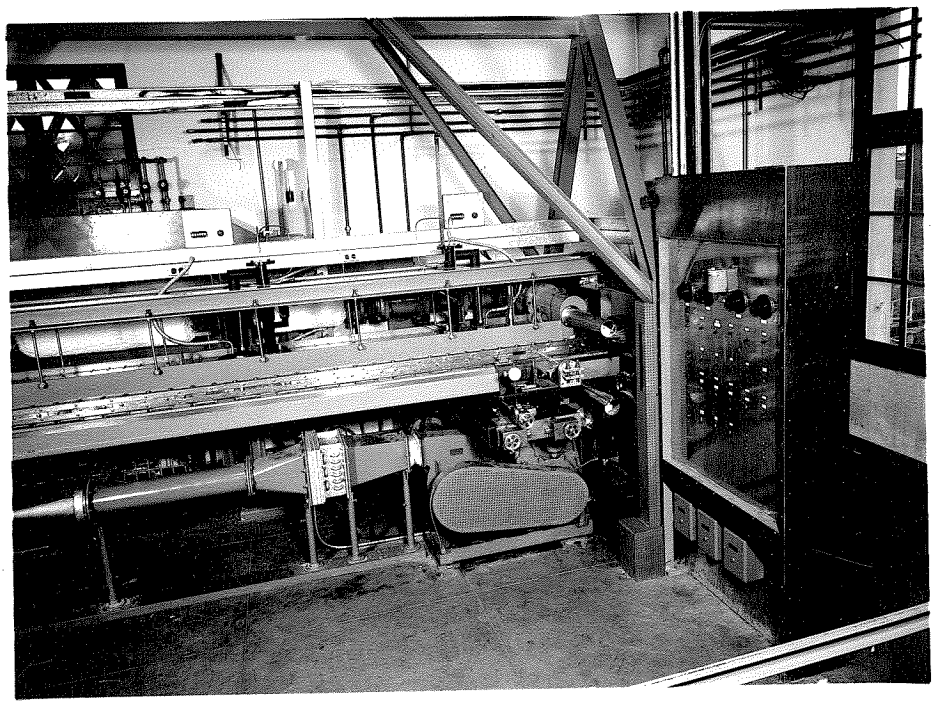

Figure 3. Downstream End of the Apparatus

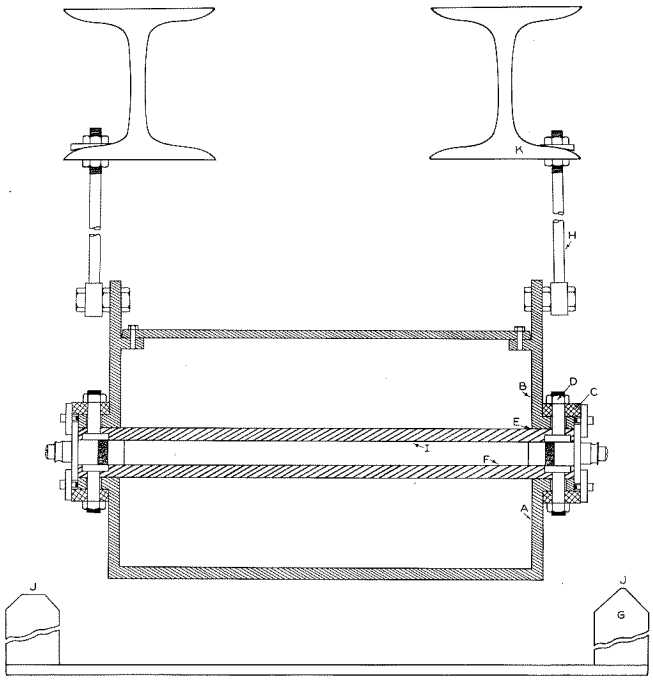

Figure 4. Sectional Drawing of Apparatus

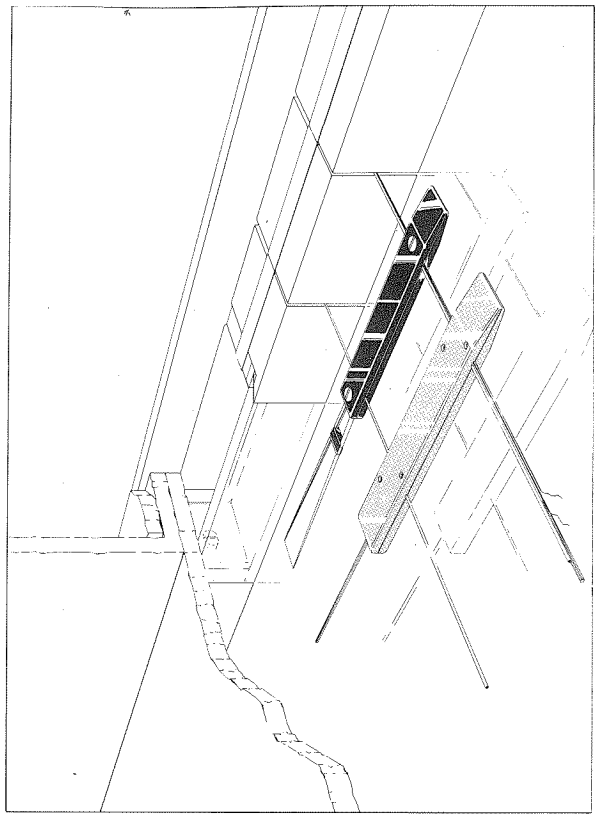

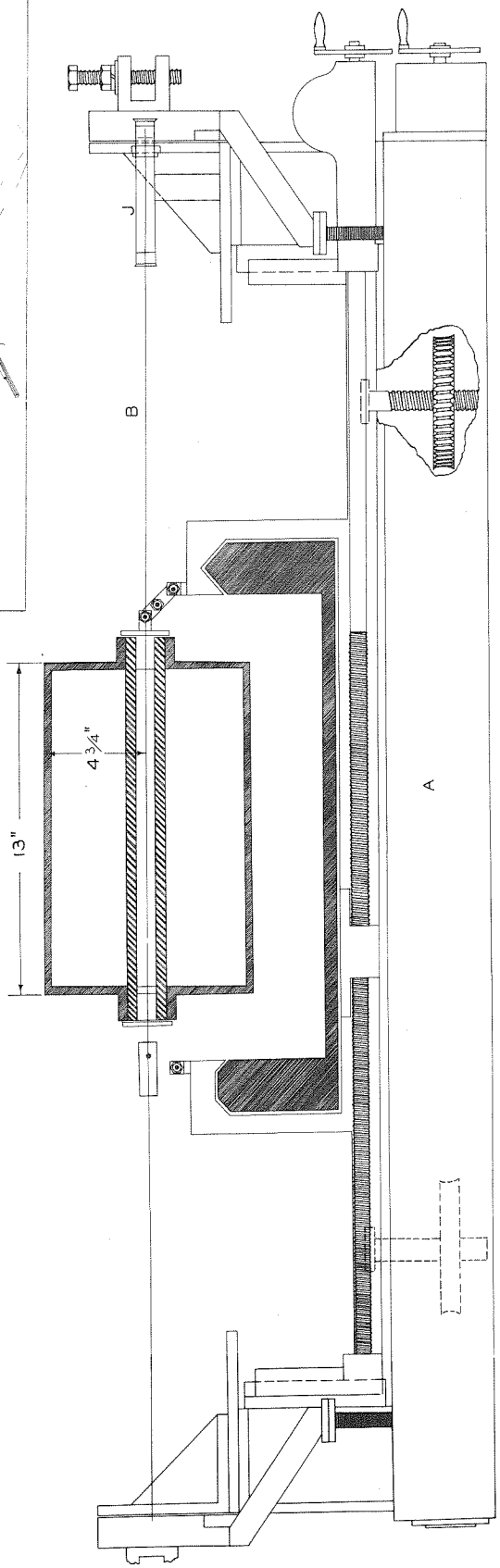

Figure 5. Drawing of Traversing Gear Showing Support of Hot Wire Anemometer

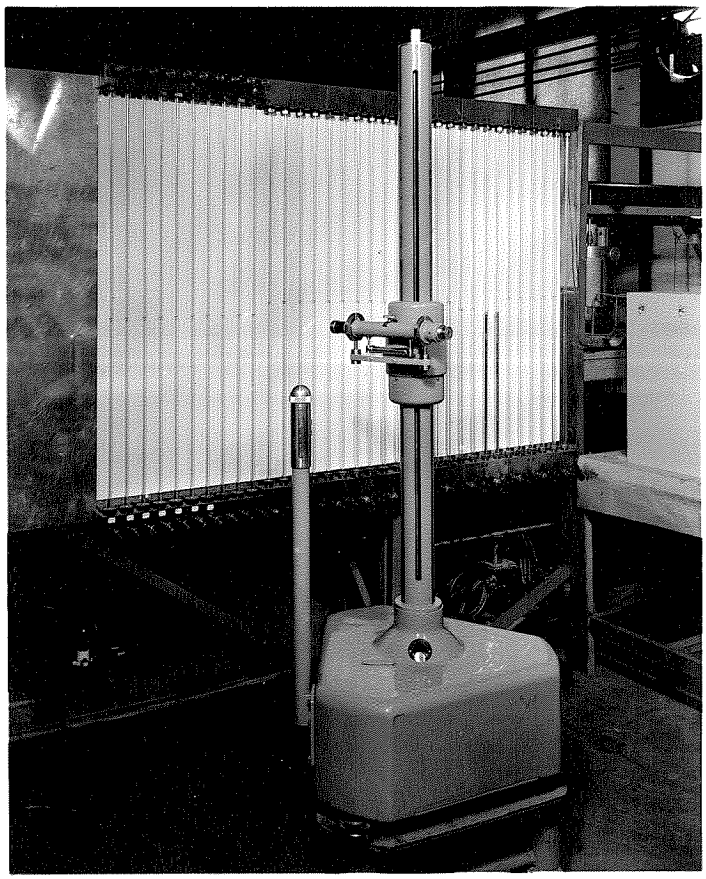

Figure 6. Cathetometer and Manometer Bank

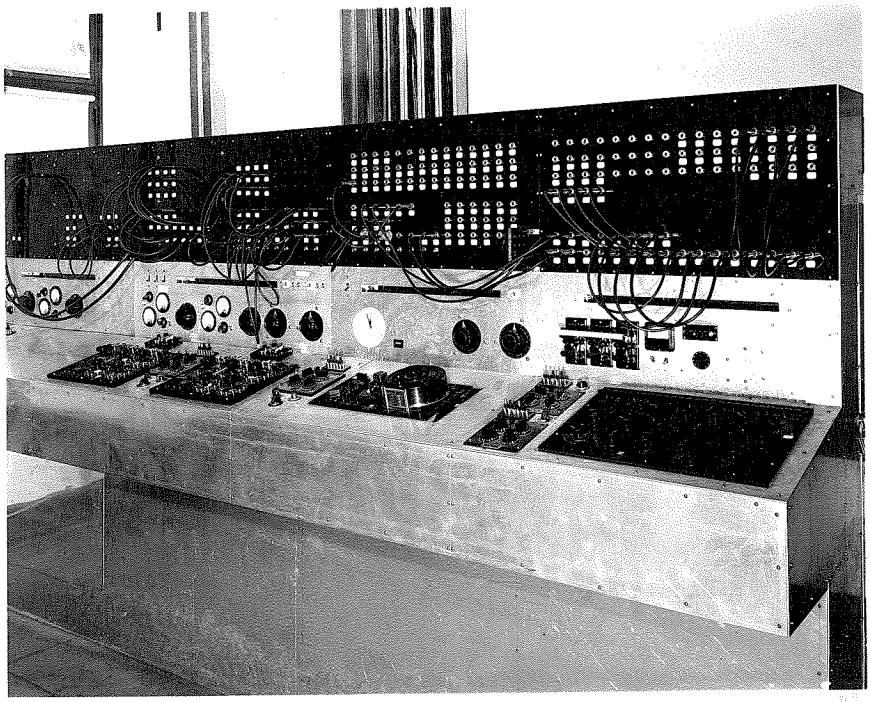

Figure 7. Temperature Bench

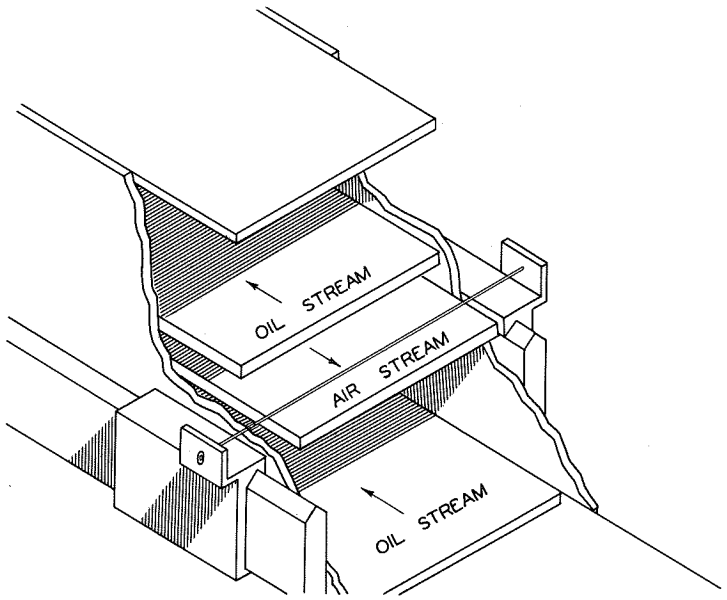

Figure 8. Schematic Drawing of Cylinder Mounted in Channel

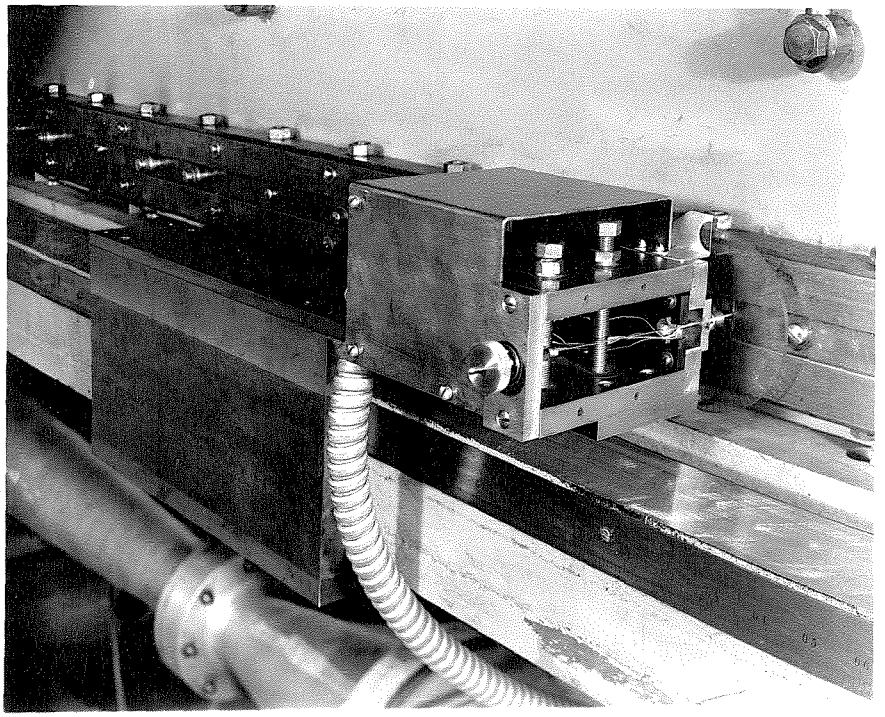

Figure 9. South Yoke Used for Supporting Cylinder

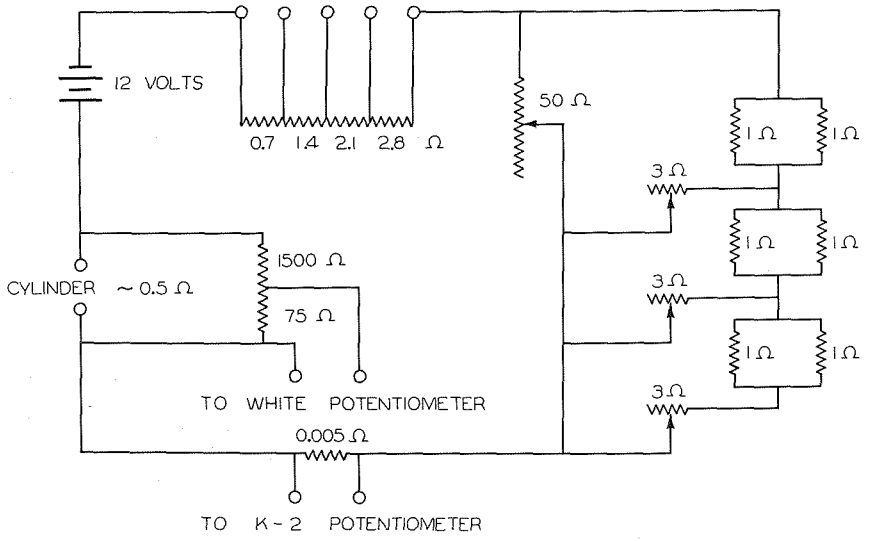

Figure 10. Cylinder Circuit Diagram

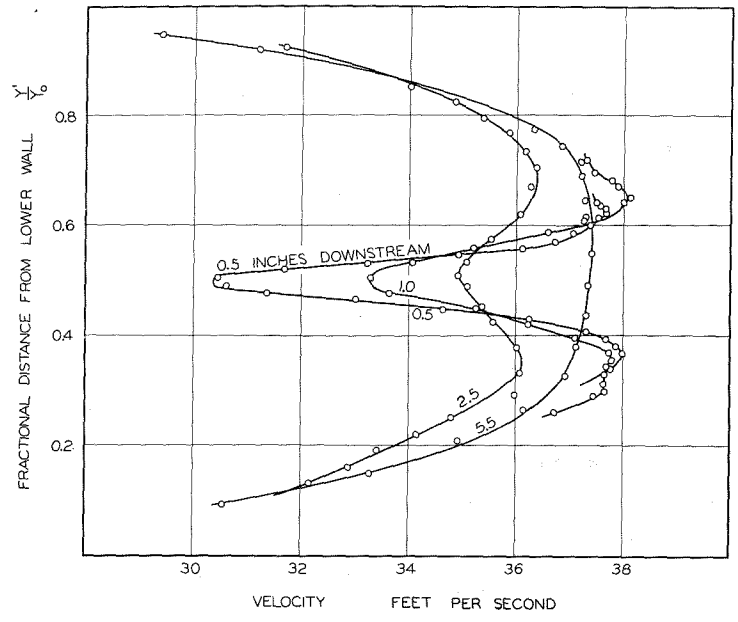

Figure 11. Specimen Air Speed Distributions at Bulk Velocity of 33.3 ft/sec

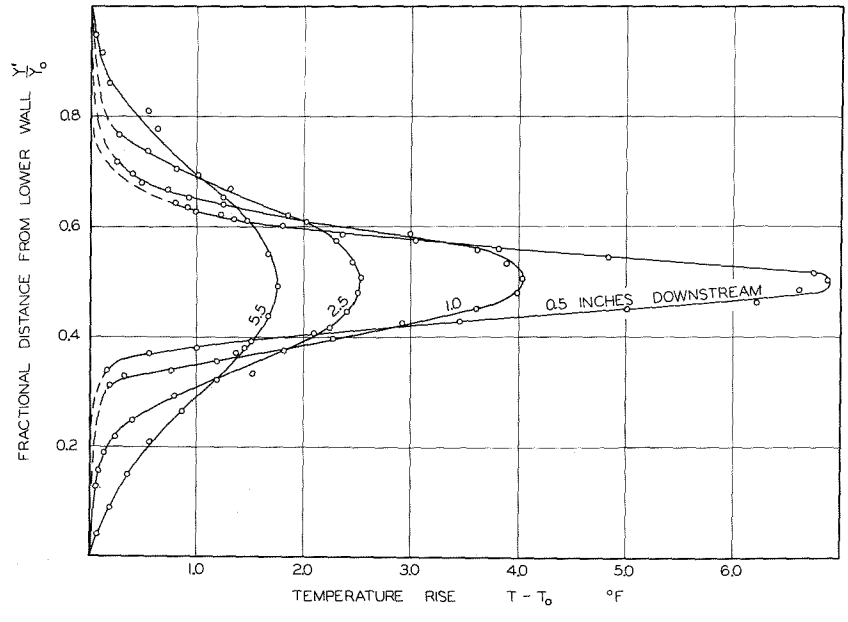

Figure 12. Specimen Temperature Distributions at Bulk Velocity of 33.3 ft/sec

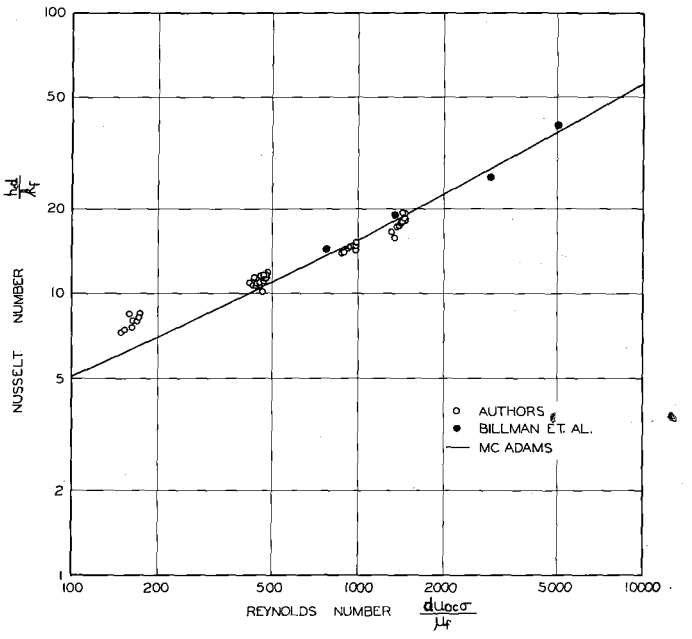

Figure 13. Nusselt number vs Reynolds number

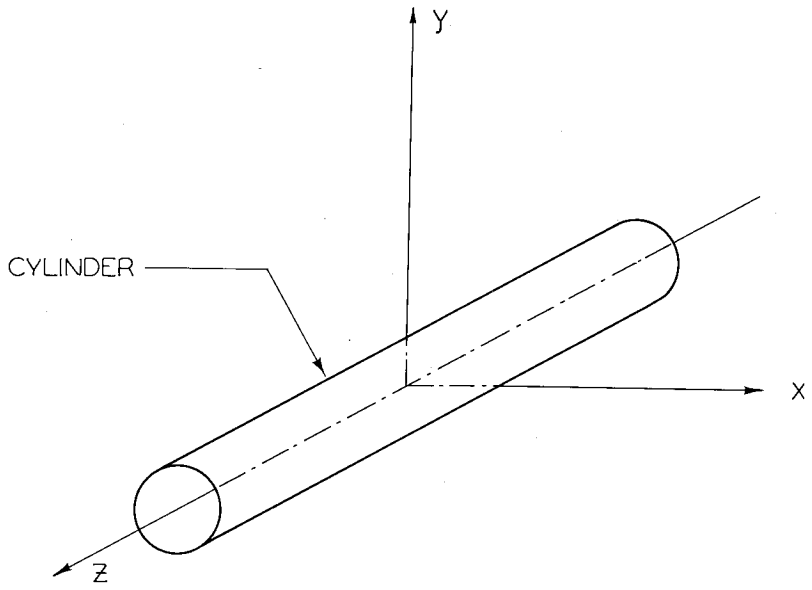

Figure 14. Coordinate System for Theory

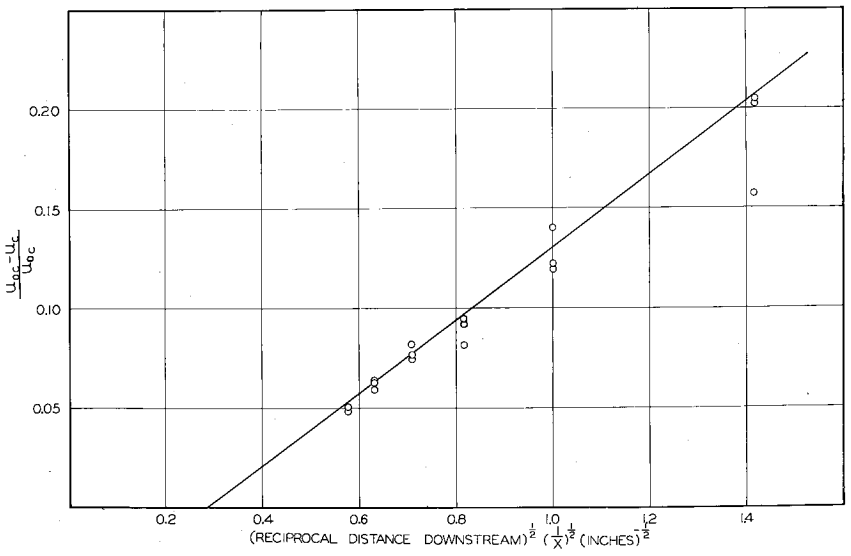

Figure 15. Variation of Centerline Velocity Deficiency with Distance Downstream from Small Cylinder

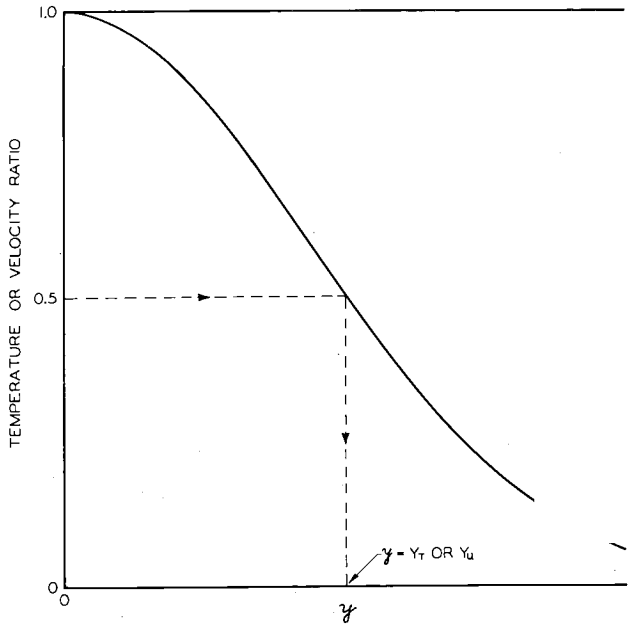

Figure 16. Method of Determination of Characteristic Width of Wake

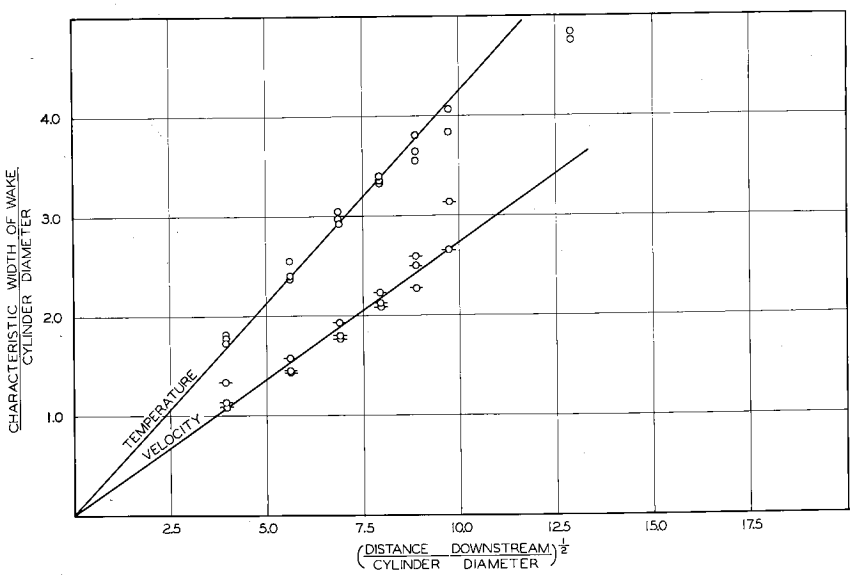

Figure 17. Variation of Characteristic Widths of Velocity and Temperature Wakes with Distance Downstream from Small Cylinder

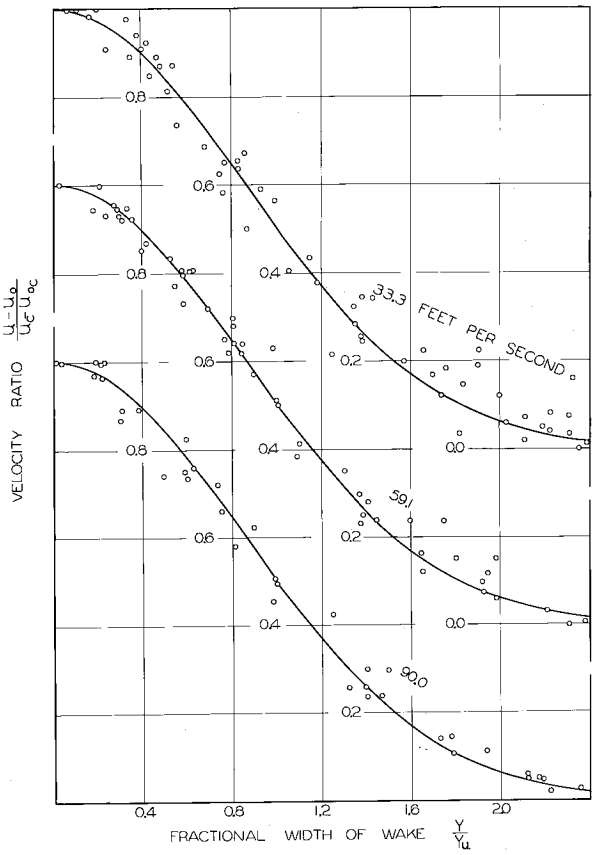

Figure 18. Comparison of Experimental Velocity Data with Theory

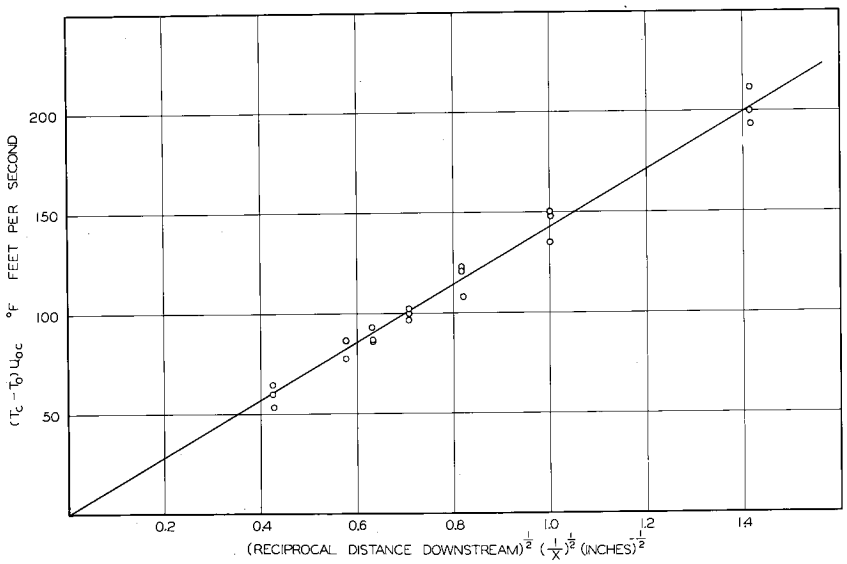

Figure 19. Variation of Centerline Temperature Rise with Distance Downstream from Small Cylinder

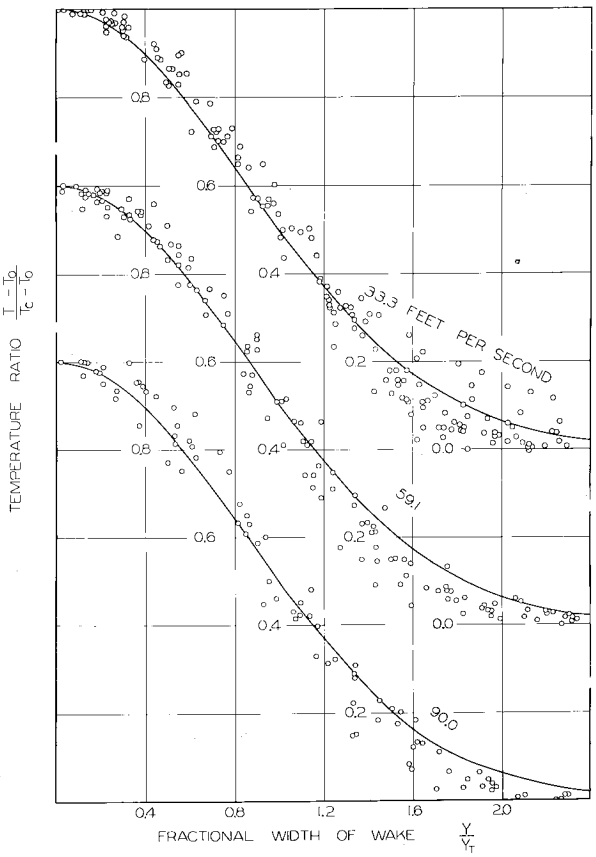

Figure 20. Comparison of Experimental Temperature Data with Theory

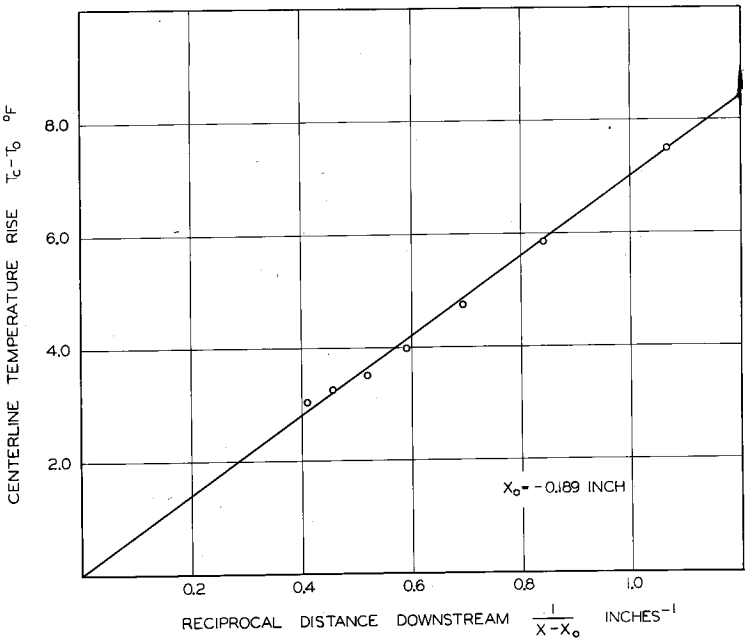

Figure 21. Variation of Centerline Temperature Rise with Distance Downstream from Sphere

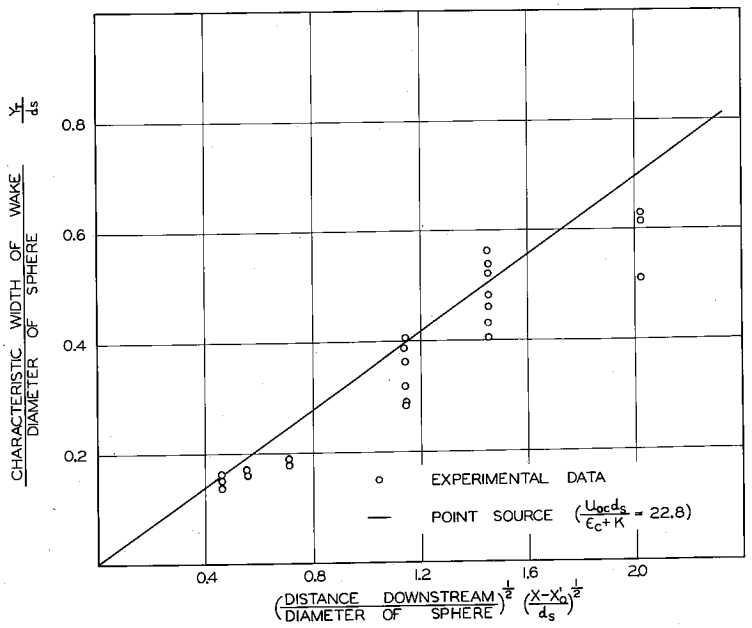

Figure 22. Variation of Characteristic Width of Temperature Wake with Distance Downstream from Sphere

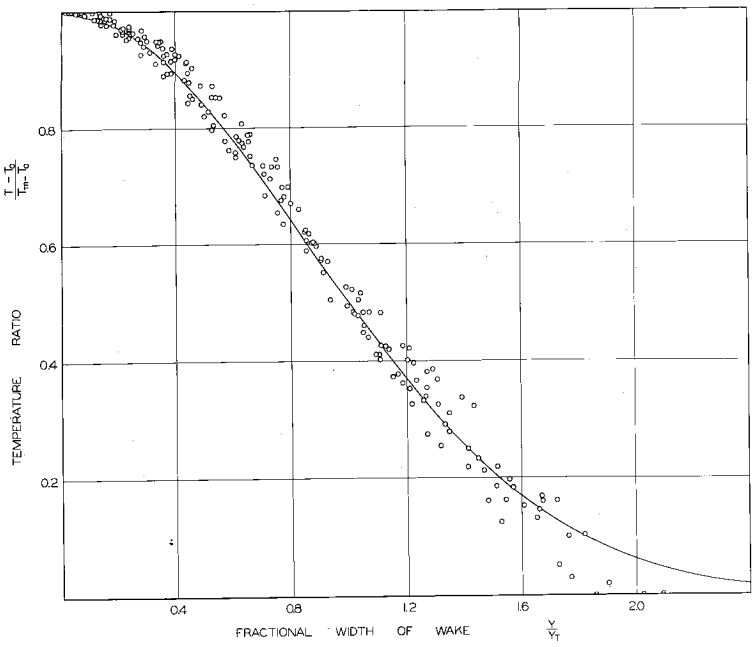

Figure 23. Comparison of Experimental Temperature Data for the Wake of Sphere with Theory

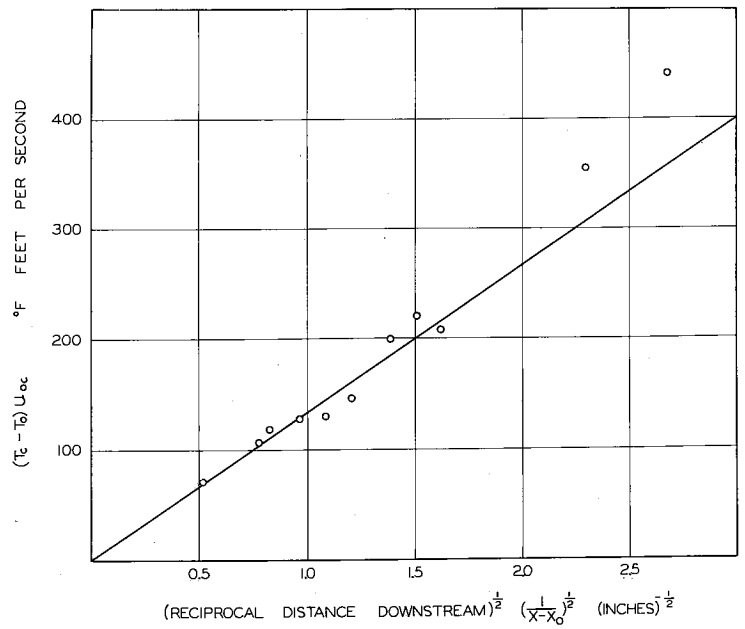

Figure 24. Variation of Centerline Temperature Rise with Distance Downstream from Large Cylinder

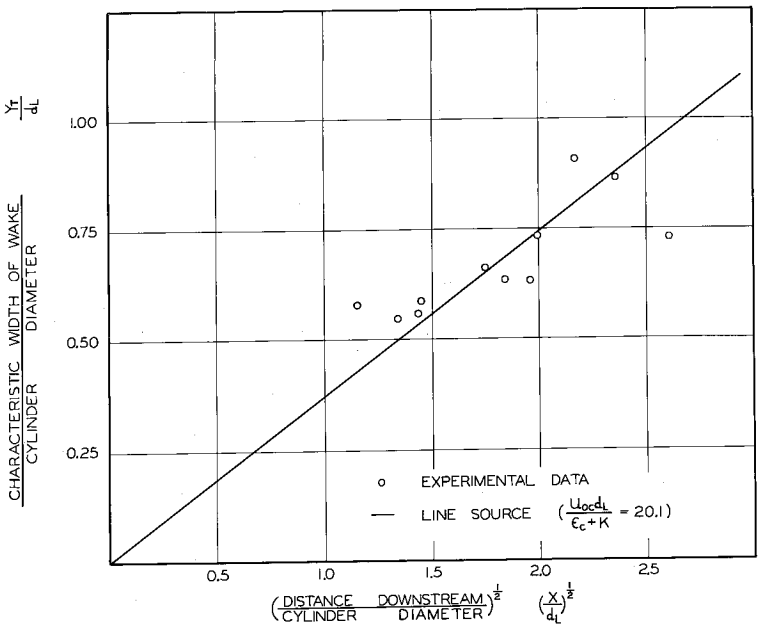

Figure 25. Variation of Characteristic Width of Temperature Wake with Distance Downstream from Large Cylinder

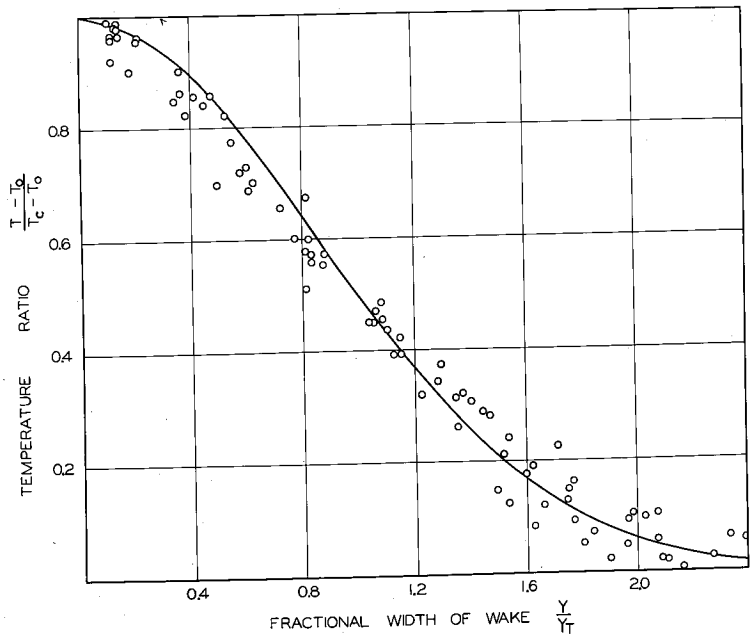

Figure 26. Comparison of Experimental Temperature Data for Wake of Large Cylinder with Theory

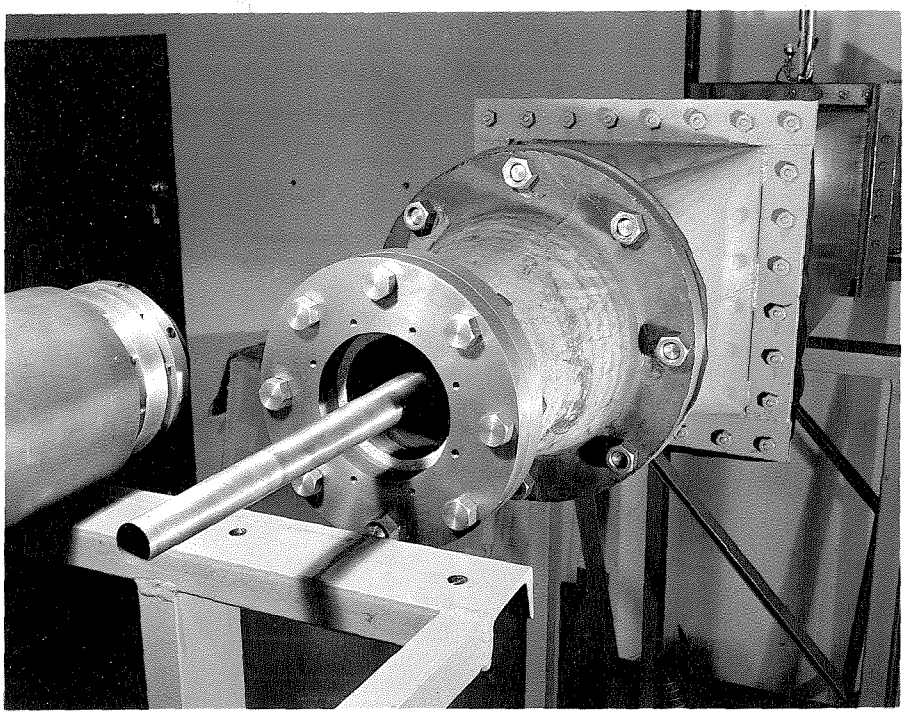

Figure 27. Turbulent Diffusion Flame Apparatus Dismantled Showing Gas Injection Tube and Annular Air Space

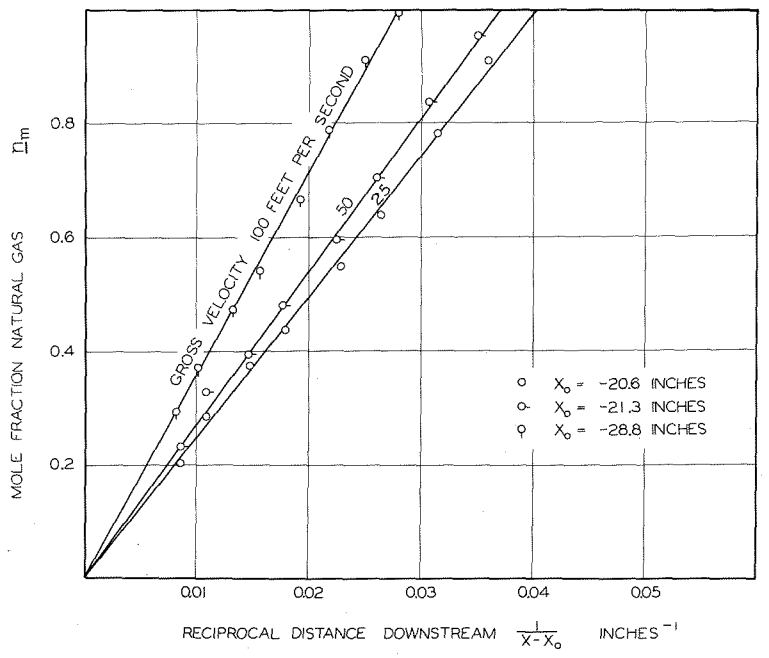

Figure 28. Variation of Maximum Mole Fraction of Natural Gas with Distance Downstream from the Exit of Gas Injection Tube

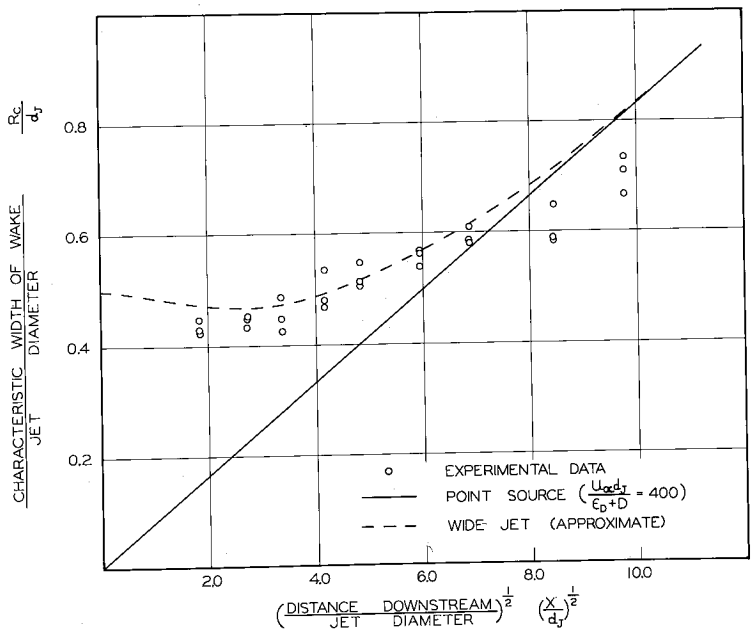

Figure 29. Variation of Characteristic Width of Concentration Wake with Distance Downstream from Exit of Gas Injection Tube

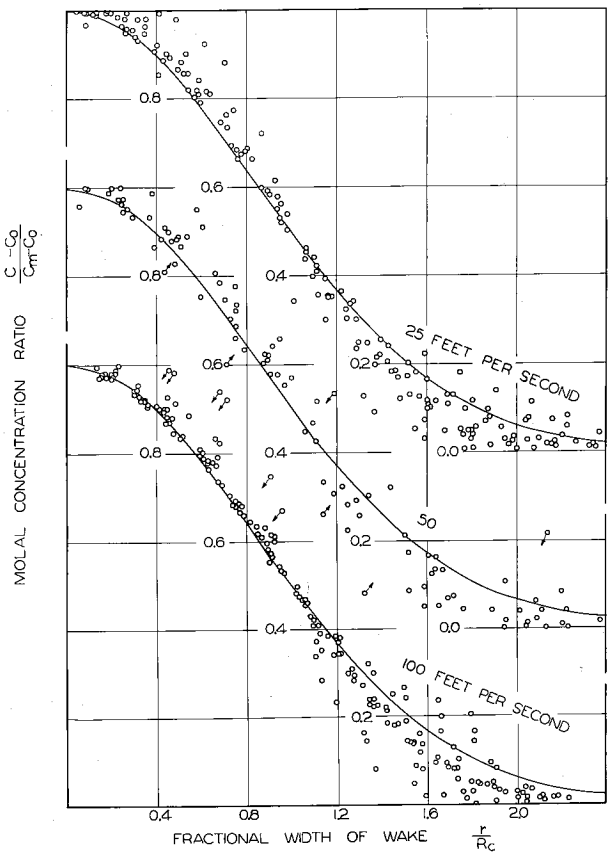

Figure 30. Comparison of Experimental Concentration Data for Diffusion Apparatus with Theory

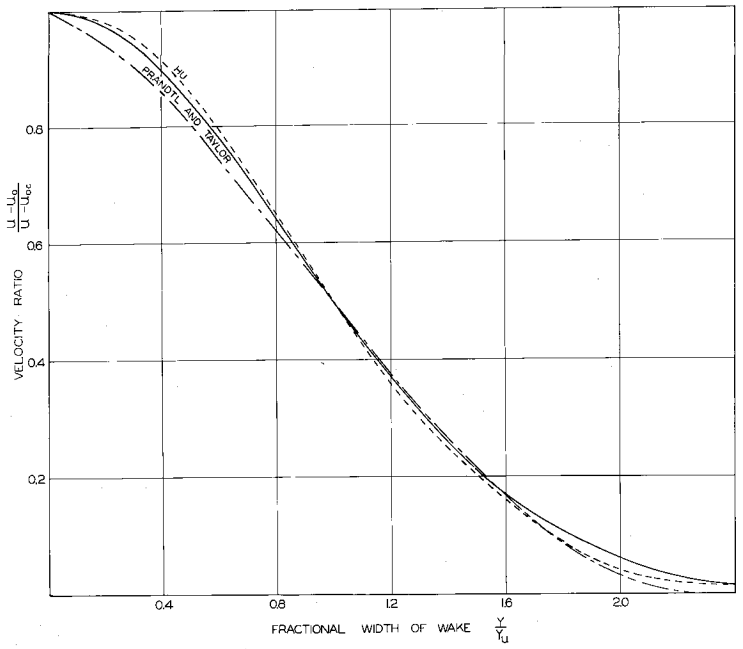

Figure 31. Comparison of Several Theoretical Velocity Distributions with Present Theory

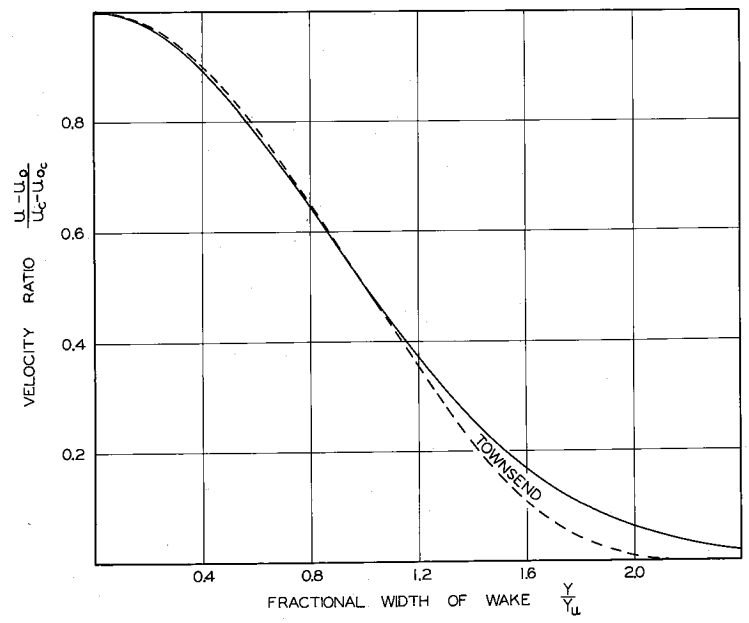

Figure 32. Comparison of Theoretical Velocity Distributions with Present Theory

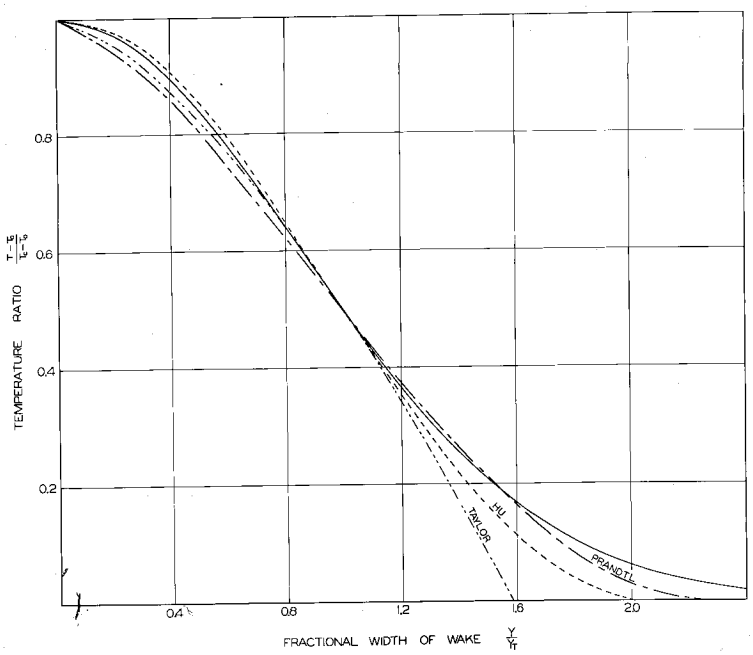

Figure 33. Comparison of Several Theoretical Temperature Distributions with Present Theory

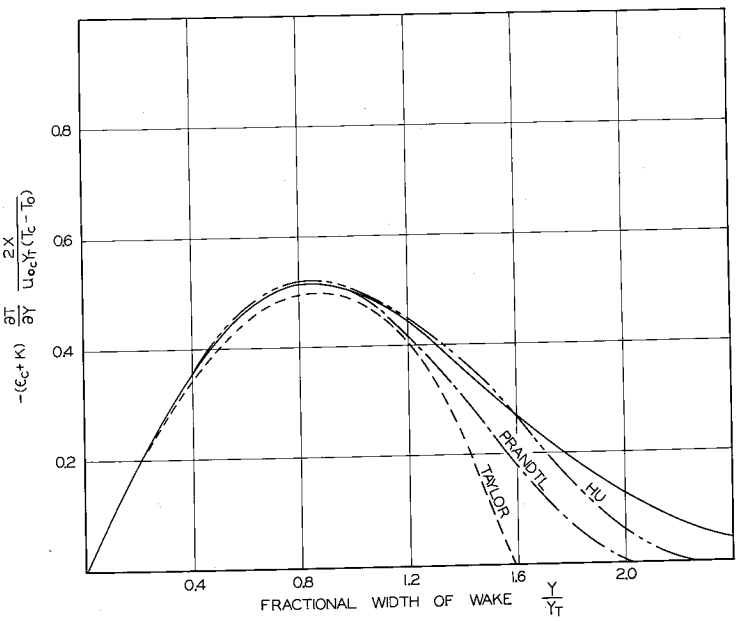

Figure 34. Comparison of Several Theoretical Heat Flux Distributions with Present Theory

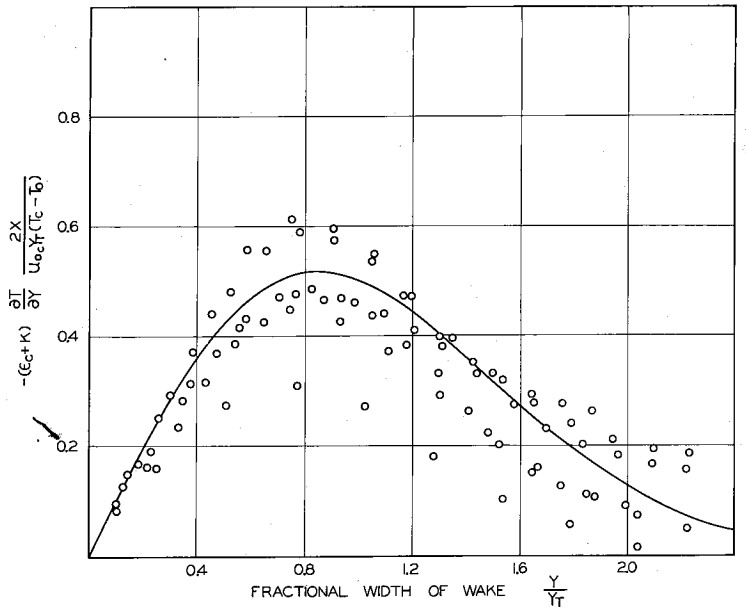

Figure 35. Comparison of Heat Flux Calculated from Experimental Data with Theory

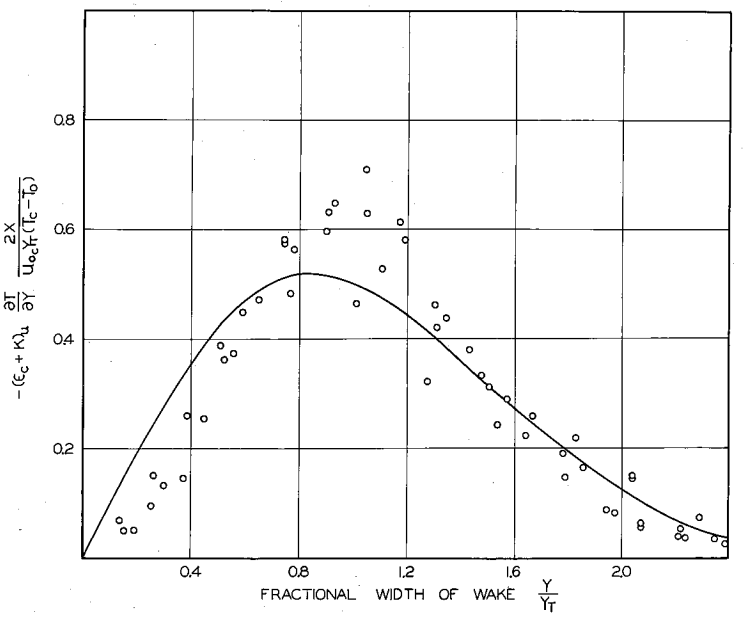

Figure 36. Comparison of Heat Flux Calculated from Uniform Flow Eddy Conductivities with Theory

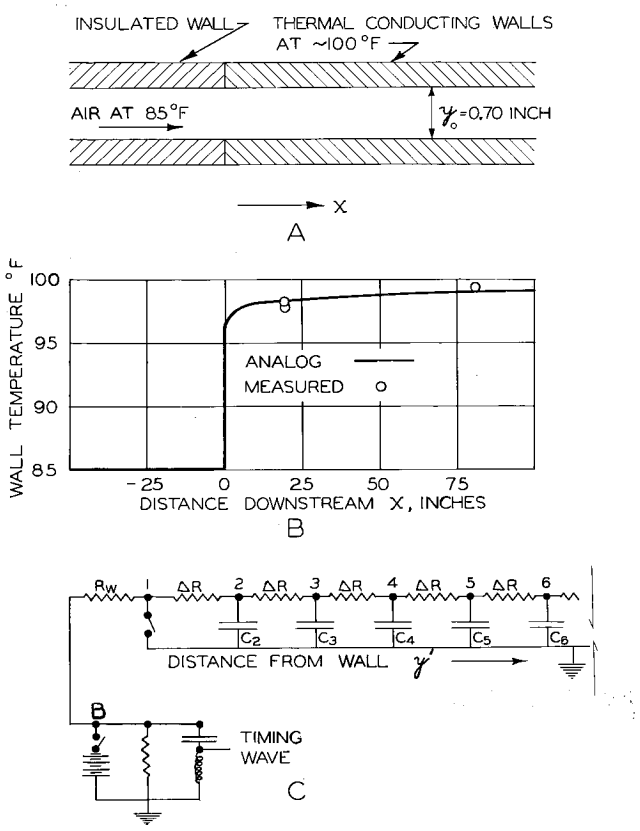

Figure 37. A Schematic Representation of Conditions at Entrance to Heated Section for Conditions 100/85/100

B Variation of Measured and Calculated Wall Temperatures with Distance Downstream for conditions 100/85/100

C Diagram of Part of Analog Computer Circuit

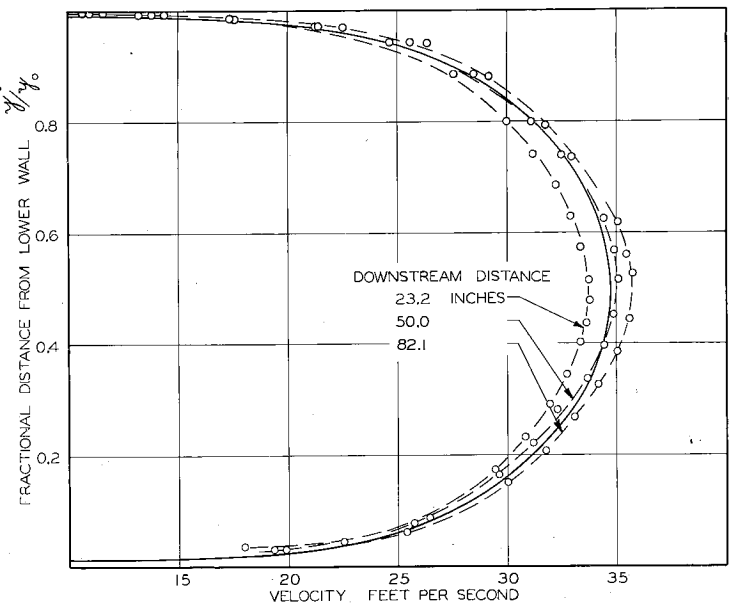

Figure 38. Experimental Velocity Distributions at Several Distances Downstream from Entrance to Heated Section

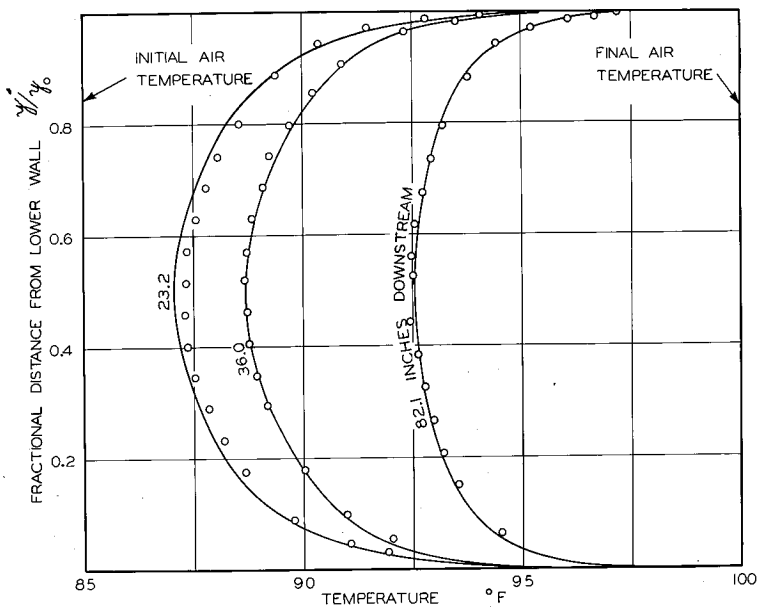

Figure 39. Comparison of Experimental and Calculated Temperature Distributions for Conditions 100/85/100

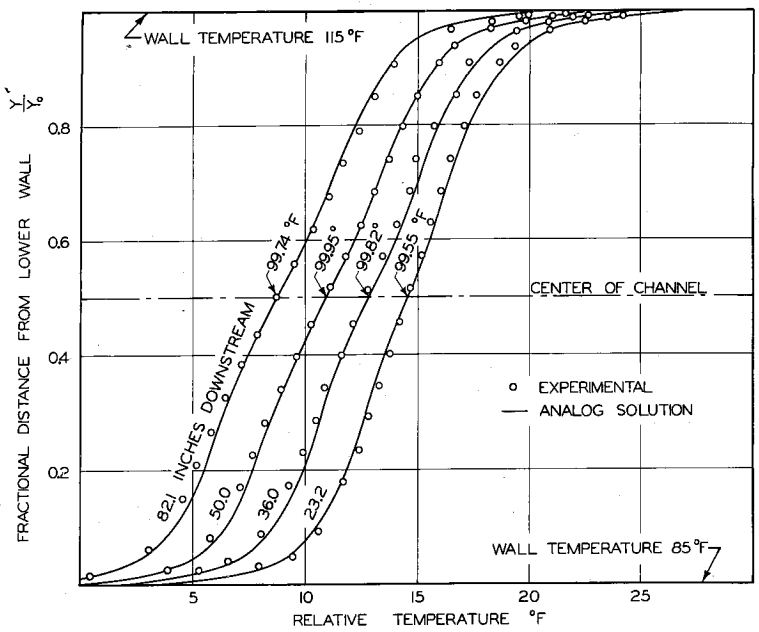

Figure 40. Comparison of Experimental and Calculated Temperature Distributions for Conditions 115/100/85

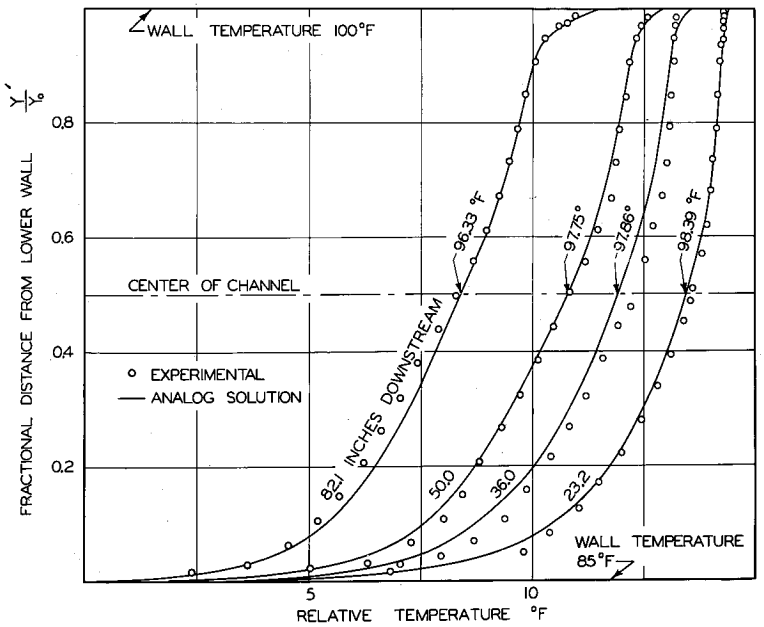

Figure 41. Comparison of Experimental and Calculated Temperature Distributions for Conditions 100/100/85

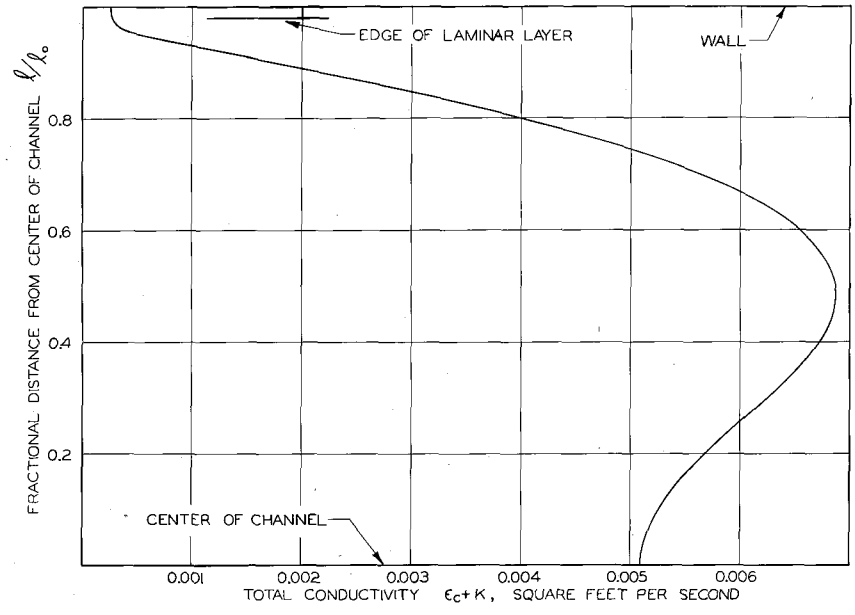

Figure 42. Variation of Eddy Conductivity with Vertical Position in Channel at Bulk Velocity of 30.5 ft/sec

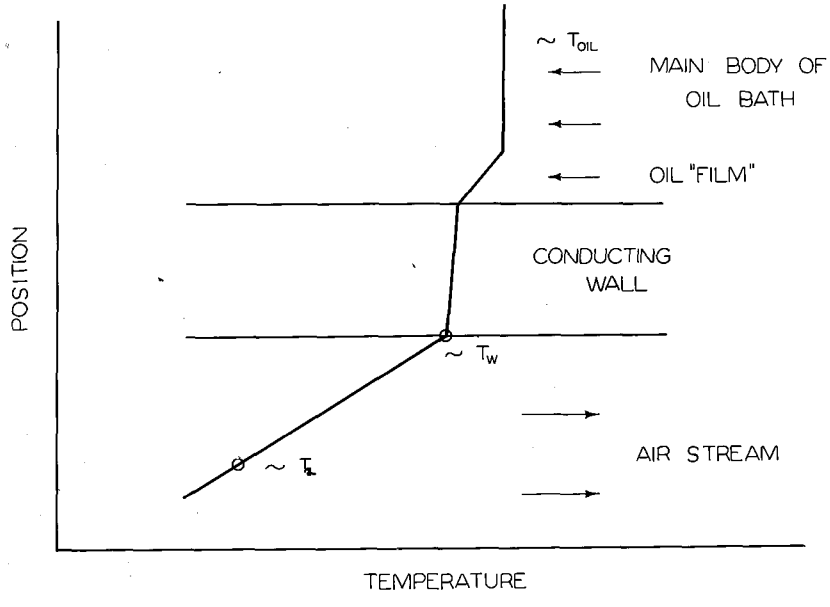

Figure 43. Schematic Representation of Conditions Existing in Vicinity of Channel Wall

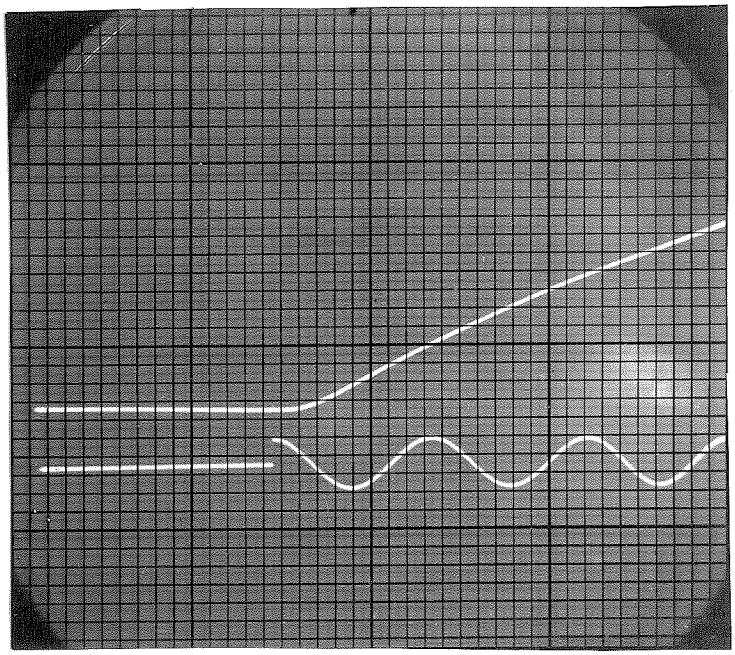

Figure 44. Specimen Oscilloscope Trace

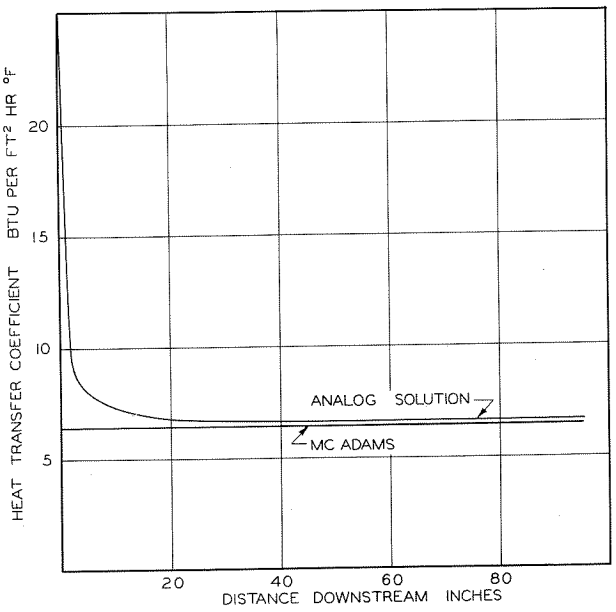

Figure 45. Variation of Local Heat Transfer Coefficient with Distance Downstream from Entrance to Heated Section

List of Tables

Table I. Temperature and Air Speed Distribution in the Wake of a Heated Cylinder

Part 1.*

y/y_o	T^a °F	u^b ft/sec	y/y_o	T °F	u ft/sec
	x = 0.50 in y_o = 0.727 in				
.340	99.41	37.8	.587	101.61	37.0
.367	99.80	38.0	.601	101.04	37.4
.381	100.24	37.8	.615	100.60	37.5
.395	100.76	37.6	.622	100.47	37.7
.408	101.35	37.3	.629	100.22	37.7
.428	102.70	36.2	.636	100.15	37.6
.450	104.26	34.6	.642	100.04	37.5
.464	105.46	33.0			
				x = 1.00 in y_o = 0.735 in	
.477	106.18	31.4			
.486	105.84	30.6	.260	99.59	36.7
.505	106.10	30.4	.288	99.70	37.4
.519	105.98	31.7	.301	99.77	37.7
.532	103.97	33.3	.315	99.93	37.6
.546	104.08	34.9	.328	100.06	37.6
.560	103.05	36.1	.342	100.51	37.7
.574	102.28	36.7	.356	100.93	37.8

* Bulk velocity - 33.3 ft/sec
Average cylinder temperature - 282°F
Rate of dissipation of energy from cylinder - 2.692 watts/in

a Experimental temperatures uncorrected for impact effect
b Experimental air speeds corrected to average y_o, P, fluid composition, and measured weight rate

Table I, Part 1 (Cont'd)

y/y_o	T °F	u ft/sec	y/y_o	T °F	u ft/sec
	$x = 1.00$ in $y_o = 0.735$ in				
.369	101.11	37.7	.268	100.04	37.0
.397	102.03	37.1	.292	100.27	37.2
.424	102.66	36.2	.338	101.02	37.5
.451	103.33	35.2	.372	101.71	37.1
.478	103.73	33.6	.423	102.68	35.8
.505	103.79	33.1	.465	103.13	34.8
.533	103.61	34.0	.506	103.16	34.5
.560	103.35	35.2	.543	103.02	35.0
.587	102.73	36.6	.592	102.46	36.2
.614	101.76	37.3	.633	101.64	37.0
.642	100.99	38.0	.677	100.88	37.3
.655	100.66	38.1	.717	100.36	37.3
.669	100.47	37.9	.746	100.13	36.7
.682	100.22	37.8	.773	100.05	36.4
.696	100.15	37.5	.800	100.00	36.0
.718	99.99	37.3	.827	99.97	35.4
			.861	99.99	34.8
	$x = 1.5$ in $y_o = 0.708$ in				
.180	99.86	34.8		$x = 2.00$ in $y_o = 0.701$ in	
.210	99.83	35.7	.168	99.73	
.239	99.92	36.4	.225	99.84	

Table I, Part 1 (cont'd)

y/y_o	T °F	u ft/sec	y/y_o	T °F	u ft/sec
	x = 2.00 in y_o = 0.701 in			x = 2.50 in y_o = 0.694 in	
.253	99.97		.133	99.78	32.2
.282	100.27		.162	99.80	32.9
.310	100.57		.190	99.85	33.4
.367	101.44		.220	99.96	34.1
.424	102.25	35.8	.249	100.12	34.8
.453	102.55	35.4	.288	100.51	36.0
.481	102.69	35.1	.335	101.04	36.1
.516	102.69	35.1	.378	101.54	36.0
.539	102.64	35.3	.422	101.96	35.6
.567	102.50	35.8	.450	102.12	35.4
.624	101.77	36.8	.479	102.24	35.0
.681	100.99	37.1	.508	102.26	34.9
.710	100.64	37.0	.537	102.18	35.0
.738	100.35	36.8	.576	102.02	35.5
.767	100.14	36.2	.623	101.56	36.1
.792	100.01	36.1	.670	101.03	36.3
.819	99.95	35.5	.708	100.54	36.4
.845	99.96	34.8	.737	100.25	36.2
.881	99.94	33.8	.768	99.99	35.8
.909	99.94	32.5	.796	99.79	35.4

Table I, Part 1 (cont'd)

y/y_o	T °F	u ft/sec	y/y_o	T °F	u ft/sec
	$x = 2.50$ in $y_o = 0.694$ in				
.825	99.70	34.8	.858	99.97	33.6
.853	99.59	34.0	.887	99.93	32.5
.912	99.49	31.7	.916	99.89	31.3
			.945	99.88	29.2
	$x = 3.00$ in $y_o = 0.697$ in		.973	99.83	24.3
.141	100.00	32.3			
				$x = 5.50$ in $y_o = 0.705$ in	
.170	100.01	33.3			
.199	100.02	33.9	.019	99.97	13.2
.256	100.40	35.9	.095	100.13	30.6
.313	100.93	36.3	.150	100.29	33.3
.371	101.52	36.3	.209	100.50	34.9
.428	101.99	35.9	.265	100.80	36.1
.486	102.22	35.8	.322	101.13	36.8
.543	102.18	35.6	.380	101.43	37.1
.600	101.86	36.2	.436	101.61	37.3
.658	101.41	36.6	.492	101.68	37.3
.715	100.82	36.4	.549	101.59	37.4
.744	100.56	36.1	.607	101.39	37.2
.772	100.33	35.8	.648	101.18	37.3
.801	100.16	35.1	.691	100.94	37.2
.830	100.04	34.5	.719	101.13	37.2

Table I, Part 1 (cont'd)

y/y_o	T ^oF	u ft/sec
	x = 5.50 in y_o = 0.705 in	
.748	100.95	36.9
.776	100.56	36.3
.804	100.47	34.9
.861	100.12	34.9
.918	100.05	31.2
.946	99.97	29.4
.975	99.93	23.1
.989	100.00	16.0

Table I, Part 2*

y/y_o	T^a °F	u^b ft/sec	y/y_o	T °F	u ft/sec
	$x = 0.50$ in $y_o = 0.696$ in				
.255	100.03	66.0	.657	100.07	67.8
.284	99.97	67.4	.686	99.95	67.0
.312	100.01	67.3	.725	99.97	64.6
.341	100.04	68.4	.743	99.95	65.8
.370	100.42	68.3			
.399	100.98	67.1		$x = 1.00$ in $y_o = 0.681$ in	
.427	101.92	65.1	.216	100.00	63.0
.456	102.51	60.4	.260	100.03	64.2
.470	102.80	58.3	.304	100.07	65.8
.485	102.90	56.6	.326	100.18	65.7
.499	102.95	55.7	.326	100.15	65.8
.514	102.87	56.3	.348	100.50	66.5
.542	102.57	60.4	.377	100.92	65.9
.571	101.57	65.7	.407	101.42	64.9
.594	100.97	66.7	.436	101.85	62.6
.628	100.34	67.5	.451	101.98	61.3

* Bulk velocity - 59.1 ft/sec
Average cylinder temperature - 242°F
Rate of dissipation of energy from cylinder - 2.692 watts/in

[a] Experimental temperatures uncorrected for impact effect
[b] Experimental air speeds corrected to average y_o, P, fluid composition, and measured weight rate

Table I, Part 2 (cont'd)

y/y_o	T °F	u ft/sec	y/y_o	T °F	u ft/sec
	$x = 1.00$ in $y_o = 0.681$ in				
.465	102.13	60.3	.441	101.56	64.0
.480	102.19	59.0	.470	101.67	64.0
.495	102.29	58.3	.470	101.71	62.9
.509	102.28	58.3	.485	101.71	62.1
.524	102.25	58.6	.500	101.81	62.6
.554	102.06	60.7	.514	101.76	62.4
.583	101.55	63.9	.529	101.77	63.0
.612	101.17	64.8	.543	101.75	63.8
.656	100.46	66.0	.558	101.57	64.5
.700	100.10	65.9	.602	101.25	66.7
.744	100.02	64.2	.646	100.78	67.6
.788	99.97	62.6	.689	100.34	67.6
			.733	100.06	66.4
	$x = 1.50$ in $y_o = 0.685$ in		.762	100.00	65.8
.222	100.01	64.0	.821	99.93	62.9
.266	100.07	66.0			
.310	100.24	66.7		$x = 2.00$ in $y_o = 0.680$ in	
.354	100.70	67.0	.144	99.97	59.4
.383	100.99	66.7	.203	99.98	62.5
.412	101.31	65.7	.232	100.04	63.8
.427	101.46	64.4	.262	100.18	65.6

Table I, Part 2 (cont'd)

y/y_o	T °F	u ft/sec	y/y_o	T °F	u ft/sec
	x = 2.00 in y_o = 0.680 in				
.291	100.31	66.7	.214	100.02	64.2
.350	100.75	67.1	.243	100.13	65.2
.409	101.17	65.9	.272	100.21	66.0
.438	101.38	65.2	.301	100.40	66.4
.468	101.47	64.3	.330	100.56	66.4
.497	101.54	64.0	.359	100.78	66.0
.526	101.53	64.2	.388	100.96	65.8
.556	101.43	64.8	.417	101.12	64.3
.615	101.12	67.2	.446	101.25	63.5
.673	100.61	68.1	.476	101.32	63.0
.703	100.42	68.2	.504	101.32	62.7
.732	100.19	67.3	.534	101.32	63.0
.762	100.07	66.6	.563	101.27	63.5
.791	100.01	65.8	.592	101.14	63.9
.821	99.98	64.3	.650	100.85	65.4
.850	99.93	62.8	.679	100.63	65.4
.879	99.96	61.0	.708	100.43	65.4
.909	99.90	55.8	.737	100.29	65.2
			.766	100.20	65.3
	x = 2.50 in y_o = 0.689 in		.795	100.11	64.3
.156	99.97	61.6	.824	100.05	63.4

Table I, Part 2 (cont'd)

y/y_o	T °F	u ft/sec	y/y_o	T °F	u ft/sec
	$x = 2.50$ in $y_o = 0.689$ in				
.853	100.04	61.8	.736	100.23	65.3
.882	100.02	59.9	.765	100.08	64.5
			.794	100.00	63.8
	$x = 3.00$ in $y_o = 0.693$ in		.823	99.92	62.7
.159	99.78	59.8	.853	99.90	61.7
.217	99.88	62.5	.881	99.90	60.6
.246	100.01	63.5	.909	99.90	57.0
.273	100.11	64.1			
				$x = 5.50$ in $y_o = 0.687$ in	
.303	100.31	65.1			
.332	100.46	65.3	.024	99.73	41.5
.390	100.81	65.3	.038	99.76	46.8
.419	100.93	64.8	.067	99.78	51.3
.448	101.03	64.7	.097	99.80	54.0
.476	101.08	64.7	.155	99.87	58.2
.505	101.10	64.2	.213	100.02	60.4
.536	101.08	65.0	.271	100.17	62.8
.566	101.02	65.2	.329	100.35	64.3
.621	100.81	65.8	.392	100.55	64.8
.650	100.66	65.8	.446	100.64	65.2
.679	100.51	65.5	.504	100.74	65.2
.707	100.33	65.4	.562	100.68	65.3

Table I, Part 2 (cont'd)

y/y_o	T °F	u ft/sec
	x = 5.50 in y_o = 0.687 in	
.621	100.60	65.2
.679	100.45	65.5
.737	100.29	63.4
.795	100.12	61.7
.853	100.01	58.7
.912	99.95	54.8
.941	99.92	51.4
.970	99.91	45.8
.984	99.91	36.8

Table I, Part 3*

y/y_o	T^a °F	u^b ft/sec	y/y_o	T °F	u ft/sec
	$x = 0.50$ in $y_o = 0.693$ in				
.310	99.81	98.1	.714	100.23	97.1
.339	99.84	99.4	.743	100.23	97.3
.339	99.87	100.4			
.368	100.04	101.0		$x = 1.00$ in $y_o = 0.705$ in	
.397	100.44	100.2	.259	99.65	101.0
.426	100.97	98.2	.288	99.68	102.5
.455	101.51	93.5	.316	99.80	103.9
.483	101.78	89.1	.345	99.99	104.0
.498	101.85	87.1	.373	100.26	103.4
.512	101.82	87.2	.401	100.57	102.4
.541	101.77	91.4	.430	100.80	100.0
.570	101.44	95.3	.458	100.98	96.3
.597	101.02	99.8	.486	101.00	94.4
.625	100.64	101.3	.515	101.05	94.8
.657	100.35	101.3	.543	100.98	97.4
.685	100.22	99.7	.571	100.78	100.0

* Bulk velocity - 90.0 ft/sec
Average cylinder temperature - 220°F
Rate of dissipation of energy from cylinder - 2.692 watts/in

[a] Experimental temperatures uncorrected for impact effect
[b] Experimental air speeds corrected to average y_o, P, fluid composition, and measured weight rate

Table I, Part 3 (cont'd)

y/y_o	T °F	u ft/sec	y/y_o	T °F	u ft/sec
	$x = 1.00$ in $y_o = 0.705$ in				
.600	100.54	102.0	.573	100.67	104.9
.628	100.30	103.8	.601	100.56	105.0
.657	100.00	103.9	.630	100.35	106.0
.686	99.79	103.6	.658	100.22	106.5
.713	99.73	102.4	.687	100.03	106.8
.742	99.70	101.3	.715	99.92	105.7
.764	99.69	100.0	.744	99.77	104.5
			.772	99.73	103.4
	$x = 1.50$ in $y_o = 0.702$ in		.801	99.68	101.2
.231	99.75	99.1			
.259	99.75	100.8		$x = 2.00$ in $y_o = 0.693$ in	
.288	99.84	102.1	.155	99.70	91.9
.316	99.90	103.3	.213	99.72	96.5
.345	100.04	105.1	.242	99.77	97.6
.373	100.24	105.8	.270	99.86	99.1
.402	100.43	104.5	.299	99.98	100.0
.430	100.65	103.0	.358	100.28	99.2
.459	100.71	101.7	.415	100.57	97.3
.487	100.73	100.2	.444	100.67	96.5
.516	100.79	100.0	.472	100.79	95.4
.544	100.78	101.5	.501	100.80	94.6

Table I, Part 3 (cont'd)

y/y_o	T °F	u ft/sec	y/y_o	T °F	u ft/sec
	$x = 2.00$ in $y_o = 0.693$ in				
.530	100.79	95.5	.456	100.79	103.2
.560	100.76	97.3	.484	100.84	102.3
.617	100.57	100.2	.513	100.83	102.3
.674	100.25	101.3	.542	100.80	102.2
.703	100.12	101.1	.571	100.78	102.3
.732	100.01	100.4	.600	100.74	104.4
.761	99.95	100.2	.629	100.62	104.7
.790	99.87	98.8	.686	100.46	105.6
.819	99.85	97.2	.715	100.34	105.0
.848	99.85	95.4	.741	100.21	103.5
.905	99.83	88.8	.773	100.15	102.4
			.802	100.19	99.3
	$x = 2.50$ in $y_o = 0.693$ in		.831	100.15	96.6
.167	99.82	92.2	.860	100.08	94.5
.225	99.91	100.2	.889	100.03	90.3
.282	100.02	102.5			
.311	100.18	103.5		$x = 5.50$ in $y_o = 0.688$ in	
.340	100.29	104.5	.020	99.81	70.1
.369	100.44	104.6	.033	99.83	74.8
.398	100.57	104.8	.064	99.81	82.0
.427	100.69	104.3	.151	99.92	92.3

Table I, Part 3 (cont'd)

y/y_o	T ^oF	u ft/sec
	x = 5.50 in y_o = 0.688 in	
.266	100.09	99.6
.384	100.33	102.1
.442	100.40	102.7
.500	100.44	103.0
.558	100.39	103.8
.616	100.34	104.4
.732	100.10	101.9
.790	100.01	99.8
.849	99.95	96.4
.907	99.95	91.4
.959	99.91	82.2
.980	99.94	72.5

Table I, Part 4*

y/y_o	T^a °F	u^b ft/sec	y/y_o	T °F	u ft/sec
	x = 0.50 in y_o = 0.703 in				
.259	99.66	37.6	.600	99.73	38.8
.344	99.68	38.8	.629	99.74	39.3
.316	99.61	38.7	.657	99.72	39.3
.287	99.59	38.2	.686	99.74	39.0
.287	99.66	38.2	.714	99.73	38.5
.316	99.60	38.7			
.344	99.65	39.2		x = 1.50 in y_o = 0.693 in	
.367	99.73	39.4	.223	99.67	36.3
.401	99.72	39.0	.280	99.69	37.4
.430	99.77	37.9	.309	99.68	37.5
.458	99.73	35.5	.338	99.70	37.8
.479	99.76	33.0	.367	99.71	37.8
.486	99.75	32.4	.425	99.73	36.4
.515	99.76	32.0	.454	99.77	35.7
.543	99.80	34.9	.482	99.71	34.3
.572	99.76	37.5	.511	99.70	34.1

* Bulk velocity - 33.7 ft/sec
Average cylinder temperature - 100°F
Rate of dissipation of energy from cylinder - 0 watts/in

a Experimental temperatures uncorrected for impact effect
b Experimental air speeds corrected to average y_o, P, fluid composition and measured weight rate.

Table I, Part 4 (cont'd)

y/y_o	T ^oF	u ft/sec
	x = 1.50 in y_o = 0.693 in	
.540	99.72	34.9
.569	99.74	35.5
.598	99.73	36.5
.620	99.70	36.7
.656	99.76	37.2
.684	99.75	37.4
.713	99.73	37.4
.742	99.75	37.0
.771	99.77	36.4
.829	99.77	35.2

Table II. Heat Transfer from Cylinder as a Function of Average Cylinder Surface Temperature

Power Dissipated watts/in	Average Surface Temperature °F	Power Dissipated watts/in	Average Surface Temperature °F
u_{oc}[a] = 11.6 ft/sec			
0.295	128.5	1.732	221.5
0.587	152.0	2.240	243.7
1,178	216.8	3.056	307.0
1.786	273.2	u_{oc} = 33.6 ft/sec	
u_{oc} = 12.3 ft/sec		0.211	113.0
0.219	118.5	0.304	120.5
0.318	128.7	0.515	135.9
0.548	151.6	1.016	168.6
1.107	202.7	u_{oc} = 70.0 ft/sec	
u_{oc} = 20.2 ft/sec		0.295	114.1
0.212	113.9	0.582	130.3
0.305	124.7	1.177	161.6
0.517	139.0	1.732	190.6
1.018	170.7	2.238	216.2
u_{oc} = 33.5 ft/sec		3.058	256.4
0.582	144.0	3.593	283.5
1.177	182.1	4.162	311.3

[a] Calculated from measured weight rate of air flow

Table II. (Cont'd)

Power Dissipation watts/in	Average Surface Temperature ^{o}F
u_{oc} = 103.8 ft/sec	
0.295	111.8
1.178	153.2
1.731	177.4
4.163	278.6
u_{oc} = 104.9 ft/sec	
0.153	103.6
0.218	108.3
0.317	112.4
0.542	122.8
0.931	141.0
1.155	150.2

Table III. Circuit Elements used in Analog Computer Circuit

Node	C_n[a] microfarads	Node	C_n microfarads
2	0.02	21	0.17
3	0.04	22	0.07
4	0.07	23	0.04
5	0.17	24	0.02
6	0.33		
7	0.64		
8	1.34		
9	2.48		
10	3.29		
11	3.20		
12	2.79		
13	2.63		
14	2.79		
15	3.20		
16	3.29		
17	2.48		
18	1.34		
19	0.64		
20	0.33		

$\Delta R^a = 46$ ohms

[a] Nominal setting on computer panel

Table IV. Wall Resistors used in Analog Computer Circuit

Case	Boundary Condition	Upper Wall R_w[a] ohms	Lower Wall R_w[a] ohms
E	115/100/85	64	82
F	115/100/85	194	248
G	100/100/85	82	72
H	100/100/85	248	216
I	100/85/100	72	72
J	100/85/100	216	216

[a] Nominal setting on computer panel

Propositions

1. Townsend (1) has suggested that there exist two separate regimes of turbulent transfer in the wake of a cylinder. The more important of these has as its mechanism the production of relatively large scale jets of fluid within the highly turbulent core of the wake. An experimental method for qualitative and semi-quantitative investigation of this phenomenon is proposed.

2. No systematic investigation of the effects of intensity and scale of turbulence on the overall heat transfer characteristics of cylinders has been undertaken. It is proposed that such a study would yield interesting information which would be of value in the design of shell and tube heat exchangers.

3. The analysis of Martinelli (2) applied to the calculation of heat transfer coefficients for liquid metals flowing inside tubes involves the assumption that $\partial T/\partial x$ is independent of radial position within the tube, where T is the temperature of the fluid at a point and x is the coordinate in the direction of motion of the fluid. Such an assumption is invalid, particularly for fluids having low Prandtl numbers (liquid metals). A method of correction is proposed.

Previous attempts at prediction of heat transfer coefficients for fluids flowing inside tubes and conduits have not been successful in correlating the available experimental data for mercury (2). A new analysis is proposed which gives results that represent the available data for mercury to within the scatter of the experimental points.

4. It is sometimes necessary to determine the diameter of a circular pipe which will deliver a specified volumetric rate of flow of a fluid under an available pumping head. If the flow is known to be turbulent, the utilization of the usual friction factor vs Reynolds number chart leads to a trial and error calculation. The choice of a different set of dimensionless moduli to correlate pressure drop data for flow in pipes has the advantage of eliminating the necessity for trial and error methods of calculation.

5. Experimental data on interfacial tensions in the methane-water-AISI 316 steel system have shown that at high pressures the steel is methane-wet, whereas at low pressures the steel is water-wet (3). It should prove worthwhile to investigate the wettability of typical oil bearing sands under similar circumstances, since the results of such a study might provide more information concerning the mechanism of multiphase flow in oil reservoirs.

6. Present methods for the correlation of pressure drop attending flow through porous media are theoretically unsatisfactory (4). The determination of the characteristics of a given oil sand requires rather extensive experimentation if it is desired to obtain information outside the region in which Darcy's law applies. A more satisfactory method of correlation of data for homogeneous fluid flow is proposed, and a single curve relating the friction factor to the Reynolds number is obtained for both consolidated and unconsolidated sands.

7. It should be possible to produce three-phase alternating current from a single direct current source by the use of three spring-coupled reed vibrators.

8. It has been demonstrated that the assumption of a special breakage mechanism leads to the conclusion that the products of a size reduction process will be distributed normally with respect to the logarithm of the particle size (5). It has been observed empirically that such special distributions result from many grinding operations and from the productions of drops in nozzles. It is proposed that further study of such phenomena, by both experimental and analytical techniques, might yield information concerning the true mechanism of formation of small particles of colloidal size and larger.

9. Certain boundary value problems in physics and engineering give rise to Sturm-Liouville problems in which the calculation of eigenvalues and eigenfunctions is difficult. Although simple methods are available for the determination of the lowest eigenvalue, the computation of higher eigenvalues is often tedious. In particular, the calculation of higher eigenfunctions requires the use of a trial function which is already orthogonal to all lower eigenfunctions. An iterative method is proposed which does not require previous orthogonalization, and which in principle yields solutions of any desired accuracy.

10. The equation of state of a gaseous, monomolecular surface film, such as tridecanoic acid on water, may be calculated using a radial distribution function of the form $g(r) = \exp -V(r)/kT$ where $V(r)$ is the potential of intermolecular force for hard spheres. The effective radius of the molecule may be determined from approximate values of atomic radii (6). Spreading pressures of tridecanoic, tetradecanoic, and pentadecanoic acid films calculated according to this method represent accurately the available experimental data(7) up to the point of condensation of the films.

11. "Reynolds Wrap" has been found to have excellent heat-insulating qualities when applied as an exterior layer to the roof of a dwelling. The observed efficiency of such insulation may be explained in terms of the known variation of the equilibrium absorptivity of aluminum oxide as a function of temperature.

References

1. Townsend, A. A., Proc. Roy. Soc. London, A197, 124 (1949)

2. Martinelli, R. C., Trans. A.S.M.E., 69, 547 (1947)

3. Hough, E. W., M. J. Rzasa, and B. B. Wood, "Interfacial Tensions at Reservoir Pressures and Temperatures-Apparatus and the Water-Methane System," presented at the New Orleans meeting, A.I.M.M.E. (October, 1950)

4. Muskat, M., Physical Principles of Oil Production, McGraw-Hill (1950)

5. Epstein, B., Ind. Eng. Chem., 40, 2289 (1948)

6. Pauling, L., The Nature of the Chemical Bond, Cornell University Press (1939)

7. Adam, N. K., The Physics and Chemistry of Surfaces, Oxford University Press (1938)